

## Deriving the vibronic coupling constants of the cyclopentadienyl radical with density functional theory and $G_0W_0$

Wong Zi Cheng<sup>a)</sup> and Liviu Ungur

*Department of Chemistry, National University of Singapore, Block S8 Level 3,  
3 Science Drive 3, 117543, Singapore*

(Dated: 24 July 2020)

The vibronic coupling constants of the cyclopentadienyl radical have been calculated with  $G_0W_0$ , HF, and DFT with various exchange-correlation functionals such as PBE, PBE0, LC- $\omega$ PBE, and the non-empirically tuned LC- $\omega$ PBE\*. The vibronic coupling constants for HF and DFT were derived using the gradients of the eigenvalues of the degenerate HOMOs of the closed-shell cyclopentadienyl anion, while the gradients of the corresponding quasiparticle energy levels were used in the case of  $G_0W_0$ . The differences between the linear vibronic constants obtained using HF and DFT were found to be small, and reduced further when the  $G_0W_0$  correction is applied to HF and DFT. Finally, the linear vibronic coupling constants calculated with  $G_0W_0$  were found to agree well with the values obtained using high level wave function methods in the literature, which suggests that  $G_0W_0$  can be a useful tool towards the study of vibronic coupling.

---

<sup>a)</sup>Electronic mail: chmwzc@nus.edu.sg

## I. INTRODUCTION

The adiabatic potential energy surface<sup>1</sup> (APES) is an important concept in the study of various problems of interest in chemistry. For example, a static study of reaction mechanisms would involve mapping out the APES of the system to determine the possible pathways between the reactants and products.<sup>2-4</sup> A thorough comparison of the saddle points found on the APES would then allow one to propose a likely mechanism for the reaction of interest. Other than that, studies of the protein folding process in biological systems require a precise knowledge of the energies of the system with respect to its conformational space.<sup>5-7</sup>

It is thus of great interest to be able to determine the APES of a chemical system accurately. Ideally, the basis of ‘accuracy’ in the context of a computational result should be its performance with regards to experiment.<sup>8</sup> However, as an auxiliary concept in theoretical chemistry, the APES has no experimental counterpart that is directly measurable. Instead, the gradient and curvature of the APES have to be related to spectroscopic observables to ascertain the accuracy of the computed APES. In particular, the derivatives of the APES along the normal modes of a molecule is equivalent to the vibronic coupling, or the coupling between a molecule’s electronic and vibrational motion.<sup>9-11</sup> Hence, the aim of this work is to examine the use of computation towards the calculation of vibronic coupling constants.

Computationally, vibronic coupling constants have been derived using density functional theory (DFT),<sup>12-21</sup> Hartree-Fock (HF),<sup>22,23</sup> and post HF methods such as complete active space self-consistent field (CASSCF),<sup>20,24-32</sup> equation-of-motion ionization potential coupled-cluster singles and doubles (EOMIP-CCSD).<sup>33-35</sup>, or multireference configuration interaction (MRCI).<sup>36-38</sup> Nevertheless, there exist some challenges with the use of these computational methods.

First, it is a well-known fact that HF does not account for electron correlation, *i.e.* individual electrons do not ‘see’ another individual electron within the HF method.<sup>39</sup> Because of that, the so-called HF orbital energies (strictly, the eigenvalues of the one-electron Fock operator) are overstabilised due to the neglect of inter-electronic repulsion. As a result, Koopmans’ theorem,<sup>40</sup> which states that the magnitude of the energy of the highest occupied molecular orbital (HOMO) should be equal to the ionisation potential of the molecule, usually does not hold. As the calculation of vibronic coupling constants can be directly related to the computed orbital energies (see Section II A below), this in turn implies that

the use of HF orbital energies to calculate vibronic coupling constants might be problematic.

Next, starting with a HF wave function, post HF methods attempt to alleviate the lack of electron correlation in HF by adding more terms to give a more complete treatment of electron-electron repulsion. For instance, the electronic wave function is treated using multiple Slater determinants in multireference methods such as CASSCF, instead of a single determinant in HF.<sup>39,41,42</sup> This is often necessary for systems such as diradicals or metal complexes, where HF is insufficient.<sup>43–45</sup> However, the computational cost of such methods are usually significantly higher; the cost of CASSCF scales exponentially with the system size.<sup>41,42</sup> As such, the usage of post HF methods is often limited to small and medium sized molecules.

Because of the limitations of these wave function methods, DFT is often the computational tool of choice for larger molecules. One major issue with DFT lies with the use of approximate exchange-correlation functionals within the Kohn-Sham formalism of DFT. More specifically, these approximate exchange-correlation functionals are developed by parametrising against some theoretical constraints<sup>46</sup> and/or experimental data.<sup>47–49</sup> As a result, there is often a strong dependence of the computed properties on the choice of exchange-correlation functional used, where functionals usually perform well against systems similar to those used in its parametrisation, but not necessarily for systems with a different chemical motif.<sup>50–52</sup> The issue with DFT is thus its reliability: the quality of the results obtained for the system and property of interest using a particular exchange-correlation functional cannot be known *a priori*, and each individual functional has to be tested rigorously before it can be used with some confidence.

On the other hand, there has been a growing interest in the use of Green’s function-based approaches in recent years. Many observables of interest are related to the expectation value of a one-particle operator, which can be expressed in terms of the one-particle Green’s function in turn.<sup>53–55</sup> Thus, explicit knowledge of the one-particle Green’s function would in principle allow these observables to be computed exactly. However, the one-particle Green’s function for a real system has to be obtained by solving the Dyson equation relating the interacting and non-interacting systems, which includes a self-energy term containing all electron correlation effects. Similar to the problem of the exchange-correlation functional in DFT, the exact self-energy term is unknown, and has to be treated approximately.

Hedin’s approach to this problem was to expand the self-energy in terms of the one-

particle Green’s function  $G$  and a screened Coulomb interaction  $W$ .<sup>56</sup> In contrast to the approximate exchange-correlation functionals in DFT, there is a clear physical meaning in the expansion of the self-energy in this approach, and it allows the treatment of electron correlation to be systematically improved upon by increasing the number of terms in the expansion of the self-energy. This is followed by the  $GW$  approximation, which neglects the vertex correction and considers only the first term in the expansion of the self-energy.<sup>56</sup> Making a rough comparison to the HF method, the Coulomb potential in HF is dependent upon a static dielectric constant, while the screened Coulomb potential in  $GW$  allows the polarisation of the electron cloud in the system with respect to an individual electron to be accounted for.

In practice, carrying out a fully self-consistent  $GW$  approximation is still computationally demanding, and the  $G_0W_0$  method is frequently used instead. In  $G_0W_0$ ,  $G$  and  $W$  are calculated using the eigenvalues and orbitals obtained from a mean field (HF or DFT) calculation, and the  $GW$  quasiparticle energies computed by applying a single correction to the initial set of eigenvalues.<sup>57,58</sup> Despite this simplification, the  $G_0W_0$  approach has shown some promise towards overcoming some of the aforementioned issues with the current computational approaches. As mentioned, the use of HF orbital energies to calculate the ionisation potential of a molecule usually results in a overestimation of the actual value, while for DFT a ‘pure’ exchange-correlation functional without any HF exchange results in an underestimation instead.<sup>59,60</sup> These systematic errors have been shown to be reduced upon applying the  $G_0W_0$  correction,<sup>61–67</sup> which supports the use of the  $G_0W_0$  approximation to improve upon HF or DFT calculations.

It is thus of interest to examine the applicability of the  $G_0W_0$  method towards the calculation of vibronic coupling constants. The number of studies using  $G_0W_0$  to describe vibronic coupling is still relatively limited.<sup>68–73</sup> In particular, the vibronic coupling constants of the  $C_{60}$  anion have been calculated using the  $G_0W_0$  correction to the local density approximation (LDA), and the computed results shown to agree well with those derived from experiment.<sup>18,19,68</sup> To the best of our knowledge, this is the only molecular system that has been examined to compare the vibronic coupling constants derived with  $G_0W_0$  and experiment so far. Hence, there is still a need to examine the use of  $G_0W_0$  towards describing vibronic coupling, and we will thus apply  $G_0W_0$  and DFT to calculate the vibronic coupling constants of the cyclopentadienyl radical in this work.

The cyclopentadienyl radical has been subject to a large number of experimental and theoretical studies in the context of the Jahn-Teller (JT) effect,<sup>9,15,17,22,29–32,34,74–84</sup> some of which are discussed here. Applegate *et al.* have used both high level wave function methods (CASSCF/6-31G\*) and dispersed fluorescence spectroscopy to determine the vibronic coupling constants of the cyclopentadienyl radical.<sup>30</sup> Sato *et al.* used generalised restricted HF theory and CASSCF to compute vibronic coupling constants as the matrix elements of the electronic operator of a vibronic Hamiltonian.<sup>22</sup> Zlatar and co-workers have used DFT to compute the JT stabilisation energy of the cyclopentadienyl radical.<sup>15,17</sup> Ichino *et al.* measured the photoelectron spectrum of the cyclopentadienyl anion and used EOMIP-CCSD calculations to construct a model JT potential for the cyclopentadienyl radical.<sup>34</sup> Finally, Sharma *et al.* presented a theoretical and computational framework to calculate the rotational parameters for molecules subject to a JT distortion, including the cyclopentadienyl radical.<sup>75</sup>

The abundance of previous studies looking at the cyclopentadienyl radical thus makes it an excellent test case to check the applicability of the  $G_0W_0$  approximation for the calculation of vibronic coupling constants. In addition, as the  $G_0W_0$  quasiparticle energies have been shown to be significantly affected by the exchange-correlation functional used as its starting point,<sup>61,62,65</sup> we will also examine the effect of the exchange-correlation functional on the calculated vibronic coupling constants, as well as the result of applying the  $G_0W_0$  correction on top of the DFT results.

The remainder of this paper is structured as follows. The protocol used to derive the vibronic coupling constants of the cyclopentadienyl radical and a brief overview of the  $G_0W_0$  approximation is given in the following section. Computational details are then given in Section III, followed by the results and discussion in Section IV, and concluding remarks in Section V.

## II. THEORY

### A. Vibronic coupling

We follow the protocol used by Sato and co-workers.<sup>22</sup> The Hamiltonian  $H_{mol}$  for a molecular system can be expressed as

$$H_{mol}(\mathbf{r}, \mathbf{R}) = T_n(\mathbf{R}) + T_e(\mathbf{r}) + U(\mathbf{r}, \mathbf{R}), \quad (1)$$

where  $\mathbf{R}$  and  $\mathbf{r}$  represent the nuclear and electronic coordinates of the molecule respectively,  $T_n$  and  $T_e$  are the nuclear and electronic kinetic energy operators respectively, and the  $U(\mathbf{r}, \mathbf{R})$  potential term is given as a sum of electrostatic electron-electron, electron-nuclear, and nuclear-nuclear interactions

$$U(\mathbf{r}, \mathbf{R}) = U_{ee}(\mathbf{r}) + U_{ne}(\mathbf{r}, \mathbf{R}) + U_{nn}(\mathbf{R}). \quad (2)$$

The electronic Hamiltonian  $H_e$  for the molecule is then

$$H_e(\mathbf{r}, \mathbf{R}) = T_e(\mathbf{r}) + U(\mathbf{r}, \mathbf{R}). \quad (3)$$

Within the adiabatic approximation, the electronic wave function  $\varphi_m(\mathbf{r}; \mathbf{R})$  is the solution to the electronic Hamiltonian  $H_e$ :

$$\hat{H}_e \varphi_m(\mathbf{r}; \mathbf{R}) = E_m(\mathbf{R}) \varphi_m(\mathbf{r}; \mathbf{R}), \quad (4)$$

where  $E_m(\mathbf{R})$  is the potential energy surface associated with electronic state  $m$ . The electronic Hamiltonian can then be written in terms of the electronic Hamiltonian about a set of reference nuclear coordinates  $\mathbf{R}_0$  as

$$\begin{aligned} H_e(\mathbf{r}; \mathbf{R}) &= T_e(\mathbf{r}) + U(\mathbf{r}; \mathbf{R}) \\ &= T_e(\mathbf{r}) + U(\mathbf{r}; \mathbf{R}_0) + (U(\mathbf{r}; \mathbf{R}) - U(\mathbf{r}; \mathbf{R}_0)) \\ &= H_e(\mathbf{r}; \mathbf{R}_0) + \Delta U(\mathbf{r}; \mathbf{R}). \end{aligned} \quad (5)$$

The difference between the distorted and reference nuclear coordinates for a small change in the molecular geometry can be expressed as a Taylor series in the basis of mass-weighted normal coordinates  $Q_i$  about  $\mathbf{R}_0$ .<sup>85</sup> The  $\Delta U(\mathbf{r}; \mathbf{R})$  term can then be written as

$$\begin{aligned} \Delta U &= \sum_i \left( \frac{\partial U}{\partial Q_i} \right)_{\mathbf{R}_0} Q_i + \frac{1}{2!} \sum_i \sum_j \left( \frac{\partial^2 U}{\partial Q_i \partial Q_j} \right)_{\mathbf{R}_0} Q_i Q_j + \dots \\ &= \sum_i V_i^{(1)} Q_i + \frac{1}{2!} \sum_i \sum_j V_{ij}^{(2)} Q_i Q_j + \dots, \end{aligned} \quad (6)$$

where  $i, j = 1, 2, \dots, 3N - 6$  refers to the vibrational normal modes of the molecule ( $3N - 5$  in the case of a linear molecule), and  $V_{i_1 i_2 \dots i_n}^{(n)}$  is the  $n^{\text{th}}$  order vibronic coupling constant:

$$V_{i_1 i_2 \dots i_n}^{(n)} = \left( \frac{\partial^n U}{\partial Q_{i_1} \partial Q_{i_2} \dots \partial Q_{i_n}} \right)_{\mathbf{R}_0}. \quad (7)$$

Note that only terms that are dependent on the nuclear coordinates,  $U_{ne}(\mathbf{r}, \mathbf{R})$  and  $U_{nn}(\mathbf{R})$ , appear in  $V_{i_1 i_2 \dots i_n}^{(n)}$ .

Equation (6) thus describes the coupling between the electronic and vibrational motion of a molecule. In the theory of vibronic coupling, the crude adiabatic approximation is used instead of the Born-Oppenheimer or Born-Huang adiabatic approximations;<sup>11</sup> *i.e.* the change in the electronic energy of the molecule as it is deformed from its reference structure is accounted for by the potential  $\Delta U$  term, while the electronic wave functions at  $\mathbf{R}_0$ ,  $\varphi_m(\mathbf{r}; \mathbf{R}_0)$  are used as the basis of the electronic operators in the vibronic Hamiltonian.

To calculate  $V_{i_1 i_2 \dots i_n}^{(n)}$ , we can write Equation (6) explicitly as a sum of one-electron operators and a nuclear-nuclear repulsion term, which correspond to the derivatives of  $U_{ne}$  and  $U_{nn}$  respectively. For example, the first order vibronic coupling operator with respect to a normal mode  $Q_i$  can be written as

$$\begin{aligned} \hat{V}_i^{(1)} &= - \sum_a \sum_\alpha \left[ \frac{\partial}{\partial Q_i} \left( \frac{Z_\alpha e^2}{|\mathbf{r}_a - \mathbf{R}_\alpha|} \right) \right]_{\mathbf{R}_0} + \frac{\partial U_{nn}}{\partial Q_i} \\ &= \sum_a \hat{v}_i^{(1)} + \frac{\partial U_{nn}}{\partial Q_i} \end{aligned} \quad (8)$$

with the one-electron operator

$$\hat{v}_i^{(1)} = - \sum_\alpha \left[ \frac{\partial}{\partial Q_i} \left( \frac{Z_\alpha e^2}{|\mathbf{r}_a - \mathbf{R}_\alpha|} \right) \right]_{\mathbf{R}_0}. \quad (9)$$

The indices  $a$  and  $\alpha$  runs over the electrons and nuclei respectively,  $Z_\alpha$  refers to the charge of nucleus  $\alpha$ , and  $e$  is the electronic charge. Finally, note that the nuclear repulsion term will be zero except for normal modes with the totally symmetric representation.

We now consider the system of interest in this work, the cyclopentadienyl radical,  $\text{C}_5\text{H}_5$ . The equilibrium geometry of the cyclopentadienyl anion, which has  $D_{5h}$  symmetry, is used as the reference structure  $\mathbf{R}_0$  (Figure 1). The cyclopentadienyl radical with  $D_{5h}$  symmetry has a degenerate electronic state  ${}^2E_1''$  in its ground state, and will undergo a JT distortion to lower its symmetry to the  $C_{2v}$  point group.<sup>84</sup> We will denote the two degenerate electronic

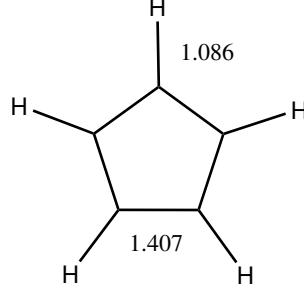


FIG. 1. PBE0/cc-pVTZ optimised structure of the cyclopentadienyl anion

states as  $|E_1''\theta\rangle$  and  $|E_1''\epsilon\rangle$ , which decompose into the  $b_1$  and  $a_2$  states respectively when the molecular symmetry is lowered from  $D_{5h}$  to the  $C_{2v}$  point group.<sup>86</sup>

The selection rules to determine which vibrational normal modes are JT active can be obtained from the symmetric product of the irreducible representations of the degenerate electronic states<sup>87</sup> as

$$E_1'' \otimes E_1'' = A_1' \oplus E_2'. \quad (10)$$

As such, only normal modes with  $a_1'$  or  $e_2'$  symmetry have a non-zero linear vibronic coupling constant, *i.e.* are linear JT active. There are a total of ten such normal modes for the cyclopentadienyl radical: two  $a_1'$  normal modes and four pairs of  $e_2'$  degenerate normal modes.

The first order vibronic coupling matrix for the  $e_2'$  normal modes can be written as

$$\mathbf{V}_i^{(1)} = \begin{pmatrix} \langle E_1''\theta | \hat{V}_i^{(1)} | E_1''\theta \rangle & \langle E_1''\theta | \hat{V}_i^{(1)} | E_1''\epsilon \rangle \\ \langle E_1''\epsilon | \hat{V}_i^{(1)} | E_1''\theta \rangle & \langle E_1''\epsilon | \hat{V}_i^{(1)} | E_1''\epsilon \rangle \end{pmatrix}. \quad (11)$$

Here, a bold  $\mathbf{V}$  is used to refer to the matrix representation of  $\hat{V}_i^{(1)}$  in the space spanned by the two degenerate electronic states  $|E_1''\theta\rangle$  and  $|E_1''\epsilon\rangle$ .

Under the Wigner-Eckart theorem,<sup>85</sup> the vibronic coupling matrix for the  $i^{\text{th}}$  pair of  $e_2'$  degenerate vibrational modes ( $e_2'(i_\theta)$  and  $e_2'(i_\epsilon)$ ) can be reduced as

$$\begin{aligned} \mathbf{V}_{e_2'(i_\theta)}^{(1)} &= \frac{1}{\sqrt{2}} \langle E_1'' \| \hat{V}_{e_2'(i)}^{(1)} \| E_1'' \rangle \begin{pmatrix} \frac{1}{\sqrt{2}} & 0 \\ 0 & -\frac{1}{\sqrt{2}} \end{pmatrix} \\ &= \frac{1}{2} \langle E_1'' \| \hat{V}_{e_2'(i)}^{(1)} \| E_1'' \rangle \begin{pmatrix} 1 & 0 \\ 0 & -1 \end{pmatrix} \end{aligned} \quad (12)$$

and

$$\begin{aligned}
\mathbf{V}_{e'_2(i_\epsilon)}^{(1)} &= \frac{1}{\sqrt{2}} \langle E_1'' | \hat{V}_{e'_2(i)}^{(1)} | E_1'' \rangle \begin{pmatrix} 0 & \frac{1}{\sqrt{2}} \\ \frac{1}{\sqrt{2}} & 0 \end{pmatrix} \\
&= \frac{1}{2} \langle E_1'' | \hat{V}_{e'_2(i)}^{(1)} | E_1'' \rangle \begin{pmatrix} 0 & 1 \\ 1 & 0 \end{pmatrix}
\end{aligned} \tag{13}$$

where  $\langle E_1'' | \hat{V}_{e'_2(i)}^{(1)} | E_1'' \rangle$  is the reduced matrix element. The vibronic coupling constant  $V_{e'_2(i)}^{(1)}$  for this pair of degenerate modes is then

$$\begin{aligned}
V_{e'_2(i)}^{(1)} &= \frac{1}{2} \langle E_1'' | \hat{V}_{e'_2(i)}^{(1)} | E_1'' \rangle \\
&= \langle E_1'' \theta | \hat{V}_{e'_2(i_\theta)}^{(1)} | E_1'' \theta \rangle \\
&= -\langle E_1'' \epsilon | \hat{V}_{e'_2(i_\theta)}^{(1)} | E_1'' \epsilon \rangle \\
&= \langle E_1'' \theta | \hat{V}_{e'_2(i_\epsilon)}^{(1)} | E_1'' \epsilon \rangle \\
&= \langle E_1'' \epsilon | \hat{V}_{e'_2(i_\epsilon)}^{(1)} | E_1'' \theta \rangle.
\end{aligned} \tag{14}$$

If the electronic wave function of the cyclopentadienyl radical is treated as a single Slater determinant, Equation (8) then allows the relevant elements of the vibronic coupling matrix to be calculated as the sum of the integrals of the one-electron operators  $\hat{v}_i^{(1)}$  over all occupied spatial orbitals  $m$ , or the orbital vibronic coupling integrals:

$$\begin{aligned}
V_{e'_2(i)}^{(1)} &= \langle E_1'' \theta | \hat{V}_{e'_2(i_\theta)}^{(1)} | E_1'' \theta \rangle \\
&= \sum_m n_m \langle \psi_m | \hat{v}_{e'_2(i_\theta)}^{(1)} | \psi_m \rangle.
\end{aligned} \tag{15}$$

Here,  $n_m$  is the occupation number of spatial orbital  $\psi_m$  in the Slater determinant  $|E_1'' \theta\rangle$ . By considering the symmetric product of the irreducible representations of the spatial orbitals, this sum can be reduced to the orbitals with  $E_1'$  and  $E_1''$  symmetry. Finally, because of the symmetry of the matrix elements in Equation (12), the orbital vibronic coupling integrals for a degenerate pair of doubly occupied orbitals cancel each other out, and do not contribute to the overall sum in Equation (15). As a result, the vibronic coupling constants can thus be reduced to the orbital vibronic coupling constants of the doubly occupied frontier orbital,

e.g.  $\psi_\epsilon$  in  $|E_1''\theta\rangle$ :

$$\begin{aligned}
V_{e_2'(i)}^{(1)} &= \langle E_1''\theta | \hat{V}_{e_2'(i\theta)}^{(1)} | E_1''\theta \rangle \\
&= \sum_m n_m \langle \psi_m | \hat{v}_{e_2'(i\theta)}^{(1)} | \psi_m \rangle \\
&= \sum_{m \in E_1' \oplus E_1''} n_m \langle \psi_m | \hat{v}_{e_2'(i\theta)}^{(1)} | \psi_m \rangle \\
&= \langle \psi_\epsilon | \hat{v}_{e_2'(i\theta)}^{(1)} | \psi_\epsilon \rangle.
\end{aligned} \tag{16}$$

Computationally, the electronic degeneracy in the neutral radical implies the necessity of using methods that account for multireference effects as well as dynamic electron correlation. Indeed, the use of single-determinant computational methods has been shown to result in symmetry-breaking in the computed electronic states of the open-shell cyclopentadienyl radical, and vibronic coupling matrices with the wrong symmetry in turn.<sup>22</sup> Therefore, instead of the cyclopentadienyl radical, we will calculate the orbital vibronic coupling constants of the two degenerate HOMOs for the cyclopentadienyl anion to derive the vibronic coupling constants of the cyclopentadienyl radical in this work.

Here, the orbitals of interest are the degenerate HOMOs of the cyclopentadienyl radical/anion (Figure 3). These are the  $\pi$ -orbitals of a highly symmetric  $D_{5h}$  system, and are energetically far from the other occupied orbitals in the system. As such, we expect that they should remain largely unchanged with respect to the addition or removal of an electron. Thus, as the orbitals for the radical and anion are largely similar to one another, the use of the orbitals obtained with calculations on the closed-shell anion should not affect the computed vibronic coupling constants significantly. In addition, unlike the neutral radical, the cyclopentadienyl anion is a closed-shell system, which allows us to avoid the problem of symmetry-breaking in DFT.<sup>88</sup>

Summarising this section, the vibronic coupling constant  $V_{e_2'(i)}^{(1)}$  has thus been derived to be

$$V_{e_2'(i)}^{(1)} = \langle \psi_\epsilon | \hat{v}_{e_2'(i\theta)}^{(1)} | \psi_\epsilon \rangle, \tag{17}$$

where the orbital vibronic coupling constant  $\langle \psi_\epsilon | \hat{v}_{e_2'(i\theta)}^{(1)} | \psi_\epsilon \rangle$  is calculated as the gradient of the Kohn-Sham orbital or  $G_0W_0$  quasiparticle energies for the closed-shell cyclopentadienyl anion..

## B. $G_0W_0$ approximation

A brief overview of the the  $G_0W_0$  method is presented here.<sup>55,63,89</sup> The Green's function for a system of non-interacting electrons treated with a single Slater determinant can be written as

$$G_{non-int}(r_1, r_2, \omega) = \sum_i \frac{\psi_i(r_1)\psi_i(r_2)}{\omega - \varepsilon_i - i\eta} + \sum_a \frac{\psi_a(r_1)\psi_a(r_2)}{\omega - \varepsilon_a + i\eta} \quad (18)$$

where  $\varepsilon$  and  $\psi$  are the one-electron eigenvalues and eigenstates respectively,  $\omega$  is the frequency with respect to a Fourier transformation of the time difference  $t_1 - t_2$ , the indices  $i$  and  $a$  refer to the occupied and unoccupied orbitals respectively, and  $\eta$  is a positive infinitesimal. Using the simplified notation  $\mathbf{1} = (\mathbf{r}_1, t_1)$ , the Green's function for an interacting system can be written with the Dyson equation:

$$G(\mathbf{1}, \mathbf{2}) = G_{non-int}(\mathbf{1}, \mathbf{2}) + \int d(\mathbf{3}\mathbf{4})G_{non-int}(\mathbf{1}, \mathbf{3})\Sigma(\mathbf{3}, \mathbf{4})G(\mathbf{4}, \mathbf{2}). \quad (19)$$

The  $\Sigma$  term contains all inter-electronic effects and is known as the self-energy term. Similar to the challenge of determining the exact exchange-correlation functional in DFT, the problem is then to find a suitable approximation for the self-energy.

Hedin's approach was to expand the self-energy perturbatively in terms of a screened Coulomb interaction  $W$ ,<sup>56</sup> with the first order term given by

$$\Sigma(\mathbf{1}, \mathbf{2}) = i \int d(\mathbf{3}\mathbf{4})G(\mathbf{1}, \mathbf{3}^+)W(\mathbf{1}, \mathbf{4})\Gamma(\mathbf{3}, \mathbf{2}, \mathbf{4}) \quad (20)$$

where  $W$  is the screened Coulomb interaction

$$W(\mathbf{1}, \mathbf{2}) = V(\mathbf{1}, \mathbf{2}) + \int d(\mathbf{3}\mathbf{4})V(\mathbf{1}, \mathbf{3})P(\mathbf{3}, \mathbf{4})W(\mathbf{4}, \mathbf{2}) \quad (21)$$

and  $\Gamma$  is the vertex function

$$\Gamma(\mathbf{1}, \mathbf{2}, \mathbf{3}) = \delta(\mathbf{1} - \mathbf{2})\delta(\mathbf{2} - \mathbf{3}) + \int d(\mathbf{4}\mathbf{5}\mathbf{6}\mathbf{7})\frac{\delta\Sigma(\mathbf{1}, \mathbf{2})}{\delta G(\mathbf{4}, \mathbf{5})}G(\mathbf{4}, \mathbf{6})\Gamma(\mathbf{7}, \mathbf{5})\Gamma(\mathbf{6}, \mathbf{7}, \mathbf{3}). \quad (22)$$

$W$  is calculated using the bare Coulomb interaction  $V(r_1, r_2) = e^2/|r_1 - r_2|$  and a polarisation term  $P$

$$P(\mathbf{1}, \mathbf{2}) = -i \int d(\mathbf{3}\mathbf{4})G(\mathbf{1}, \mathbf{3})G(\mathbf{4}, \mathbf{1}^+)\Gamma(\mathbf{3}, \mathbf{2}, \mathbf{4}). \quad (23)$$

Equations (19) to (23) are known as the Hedin equations<sup>56</sup> and have to be solved self-consistently.

Next, the  $GW$  approximation assumes the second term of the vertex function in Equation (22) to be zero, which allows Equations (20) and (23) to be simplified to

$$\Sigma(\mathbf{1}, \mathbf{2}) = iG(\mathbf{1}, \mathbf{2}^+)W(\mathbf{1}, \mathbf{2}^+) \quad (24)$$

and

$$P(\mathbf{1}, \mathbf{2}) = -iG(\mathbf{1}, \mathbf{2})G(\mathbf{2}, \mathbf{1}^+). \quad (25)$$

Within the random phase approximation, the density response function for a non-interacting system,  $\chi_0$ , is taken to be  $P$  directly, and can be calculated using Equations (18) and (25). The dielectric function  $\epsilon$  is then

$$\begin{aligned} \epsilon(\mathbf{1}, \mathbf{2}) &= \delta(\mathbf{1}, \mathbf{2}) - \int d(\mathbf{3})V(\mathbf{1}, \mathbf{3})\chi_0(\mathbf{3}, \mathbf{2}) \\ &= \delta(\mathbf{1}, \mathbf{2}) - \int d(\mathbf{3})V(\mathbf{1}, \mathbf{3})P(\mathbf{3}, \mathbf{2}). \end{aligned} \quad (26)$$

$W$  can then be obtained as

$$W(\mathbf{1}, \mathbf{2}) = \int d(\mathbf{3})\epsilon^{-1}(\mathbf{1}, \mathbf{3})V(\mathbf{3}, \mathbf{2}). \quad (27)$$

In practice, a  $GW$  calculation would start with a mean field calculation, and uses the converged orbitals and eigenvalues to compute the Green's function for the non-interacting system (Equation (18)); *i.e.* the non-interacting system is treated with a mean field calculation. From that starting point, it is then possible in principle to solve the coupled integral equations (19) and (24) to (27) self-consistently to obtain the  $GW$  self-energy of the system, albeit the process of doing so remains very computationally challenging.

The  $G_0W_0$  approach is then a further simplification to the  $GW$  approximation, and only computes the  $GW$  self-energy once. This is usually denoted as  $G_0W_0@XCF$ , where XCF is the starting point of the  $G_0W_0$  calculation; *e.g.*  $G_0W_0@PBE0$  for a calculation using the PBE0 functional as a starting point.

The molecular property of interest, the quasiparticle energies in this case, can then be calculated using the self-energy by applying first-order perturbation theory with respect to the eigenvalues of the mean-field calculation,  $\varepsilon_i$

$$\varepsilon_i^{QP} = \varepsilon_i + \langle \psi_i | \Sigma(\varepsilon_i^{QP}) - V_{XC} | \psi_i \rangle. \quad (28)$$

Here,  $V_{XC}$  is the exchange-correlation potential used in the mean-field calculation and the quasiparticle wave function is assumed to be equal to the HF or DFT wave function  $\psi_i$ .

Equation (28) can be either be solved iteratively, or linearised to give

$$\varepsilon_i^{QP} = \varepsilon_i + Z_i \langle \psi_i | \Sigma(\varepsilon_i) - V_{XC} | \psi_i \rangle, \quad (29)$$

where  $\Sigma$  is assumed to be approximately linear about the quasiparticle energy  $\varepsilon_i^{QP}$ , and the renormalisation factor  $Z_i$  is given as

$$Z_i = \left( 1 - \left( \frac{\delta \Sigma(\omega)}{\delta \omega} \right)_{\omega=\varepsilon_i} \right)^{-1}. \quad (30)$$

### III. COMPUTATIONAL DETAILS

As mentioned in Section II A, all calculations in this work were spin restricted calculations on the closed-shell cyclopentadienyl anion. The optimised  $D_{5h}$  geometry (Figure 1, C-C: 1.407 Å, C-H: 1.086 Å) and vibrational normal modes (Table I and Figure 2) of the parent cyclopentadienyl anion system was first obtained at the PBE0/cc-pVTZ<sup>90,91</sup> level of theory using Gaussian16.<sup>92</sup>

CP2K6.1<sup>93,94</sup> was then used to obtain the energies of the degenerate HOMOs of the cyclopentadienyl anion (Figure 3) as the parent system is distorted with respect to each  $e'_2$  normal mode individually, and the results fit to a polynomial (Figure 4 and Supplementary Material S1 A). A similar fitting procedure was also used with the total energy of the parent

TABLE I. Harmonic vibrational frequencies ( $\text{cm}^{-1}$ ) of the cyclopentadienyl anion normal modes  $\nu_i$  at the PBE0/cc-pVTZ level of theory

$i$	Symmetry	Frequency	$i$	Symmetry	Frequency
1	$a'_1$	1167.9	8	$e''_1$	613.9
2		3188.7	9	$e'_2$	844.3
3	$a'_2$	1269.2	10		1060.8
4	$a''_2$	660.9	11		1410.0
5	$e'_1$	1023.0	12		3138.5
6		1477.6	13	$e''_2$	628.4
7		3164.4	14		771.7

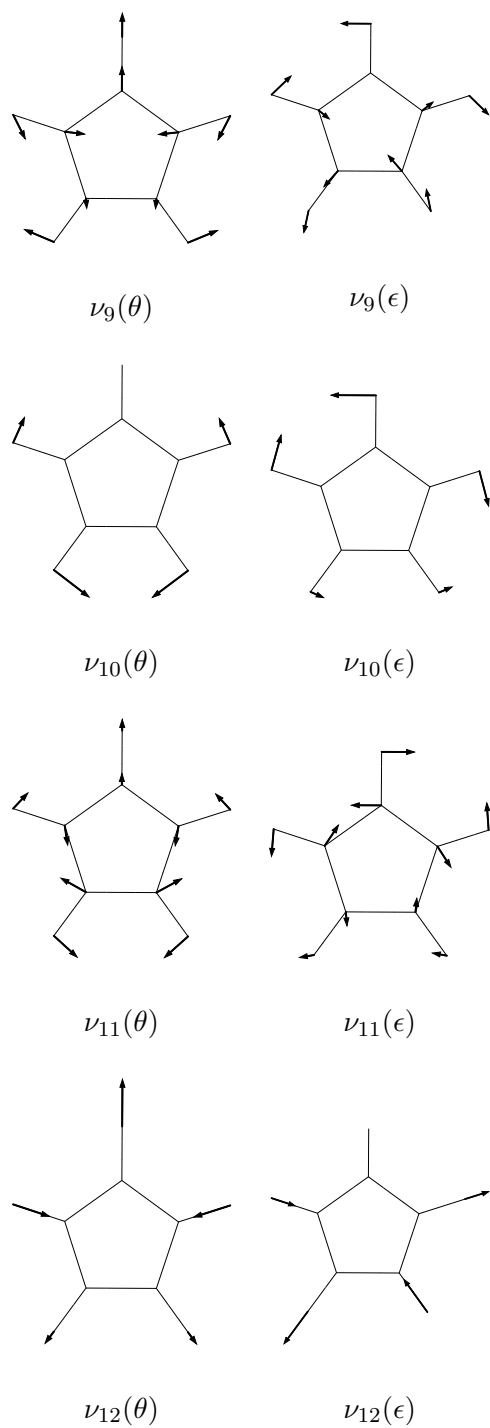


FIG. 2.  $e'_2$  normal modes of the cyclopentadienyl anion within PBE0/cc-pVTZ. Under the subduction  $D_{5h} \rightarrow C_{2v}$ , the  $e'_2$  representation is reduced to  $a_1 \oplus b_2$ .  $e'_2(\theta)$  and  $e'_2(\epsilon)$  then correspond to  $a_1$  and  $b_2$  respectively

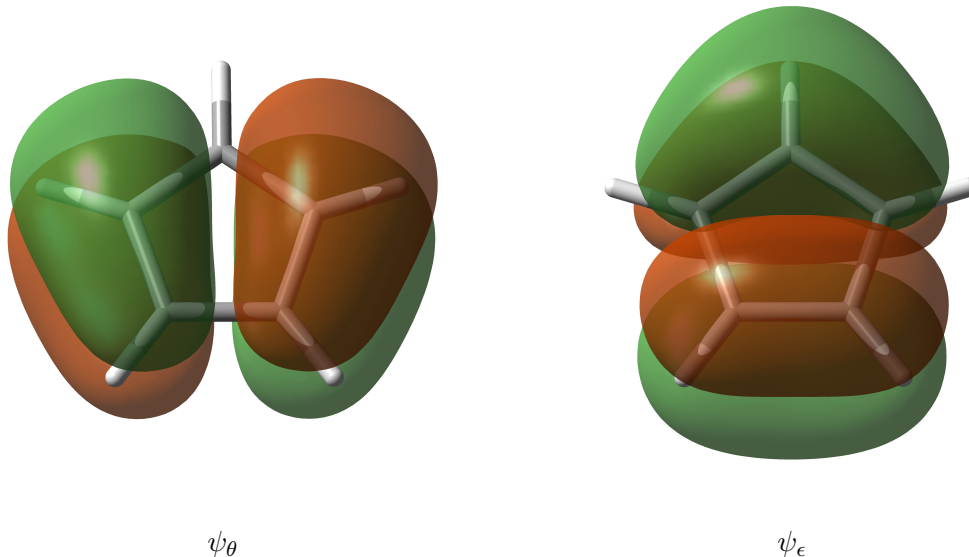


FIG. 3. Degenerate HOMOs of the cyclopentadienyl anion.  $\psi_\theta$  and  $\psi_\epsilon$  correspond to the singly occupied HOMO in the  $|E_1''(\theta)\rangle$  and  $|E_1''(\epsilon)\rangle$  electronic states of the cyclopentadienyl radical respectively.

system to obtain the frequencies of each  $e_2'$  normal mode for the exchange-correlation functionals tested in this work other than PBE0. The effect of using the optimised geometries and vibrational normal modes obtained within PBE<sup>46</sup> to determine the vibronic coupling constants was also tested, and found to be minimal (Supplementary Material S1 B).

The PBE, PBE0, LC- $\omega$ PBE<sup>95</sup>, and LC- $\omega$ PBE\* functionals, as well as HF<sup>39</sup> were used to calculate the orbital vibronic coupling constants with the cc-pVTZ basis set, where the LC- $\omega$ PBE\* functional refers to the IP-tuned LC- $\omega$ PBE functional.

In a range-separated functional, the exact exchange can be decomposed into separate short and long range components using the error function (erf).

$$\frac{1}{r_{12}} = \frac{1 - [\alpha + \beta \text{erf}(\gamma r_{12})]}{r_{12}} + \frac{\alpha + \beta \text{erf}(\gamma r_{12})}{r_{12}} \quad (31)$$

$r_{12}$  is the inter-electronic distance,  $\alpha$  is the fraction of exact exchange present in the short range, which increases to  $\alpha + \beta$  in the long range.  $\gamma$  then determines the partitioning between the short and long range regions. The parameters  $\alpha$ ,  $\beta$  and  $\gamma$  are then usually determined by parametrisation against some experimental data, and set as fixed constants defining a functional.<sup>96-98</sup>

Alternatively, it has been suggested that these range-separation parameters could be

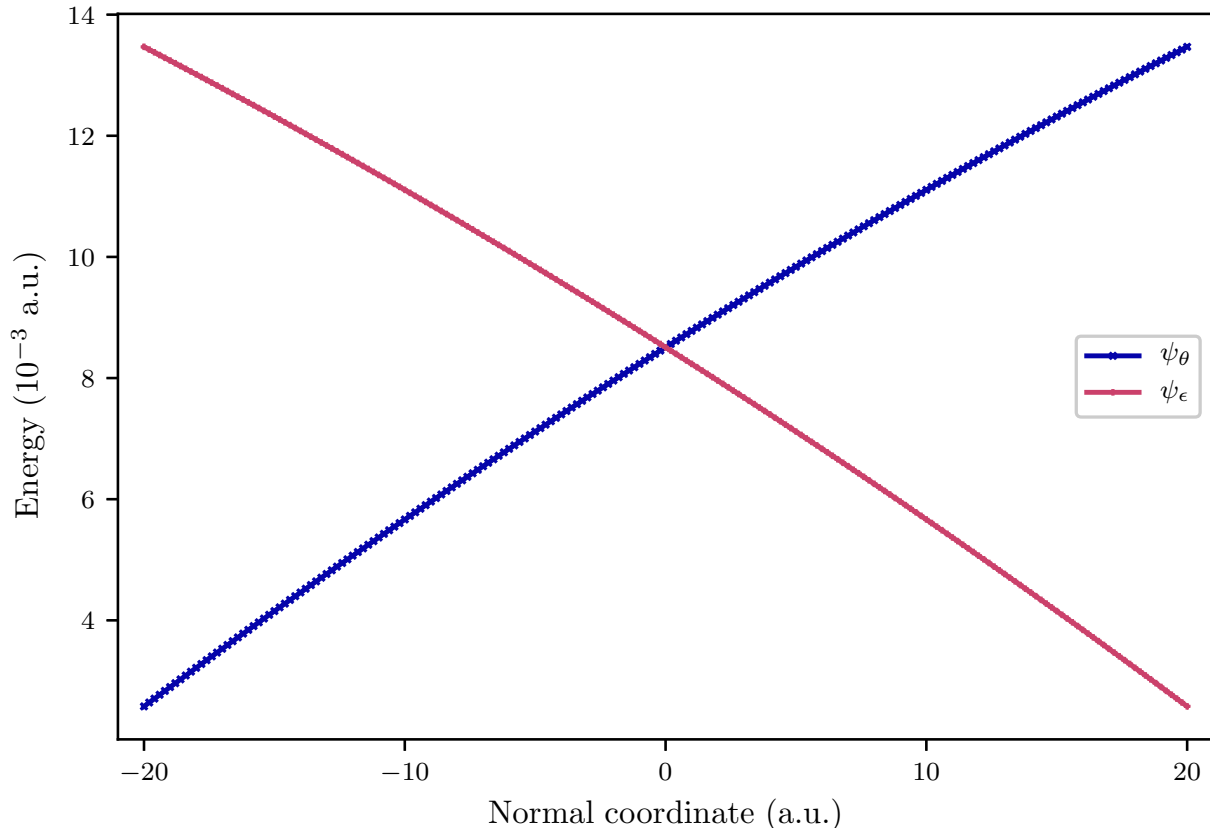


FIG. 4. PBE0 orbital energies of  $\psi_\theta$  and  $\psi_\epsilon$  with respect to the distortion along  $\nu_{10}(\theta)$ . The full set of *ab initio* results are given in Supplementary Material S1 E.

determined non-empirically for each individual molecule instead, such that the resulting calculation with the functional obeys a particular theorem or physical condition.<sup>99–102</sup> For example, in what is known as IP-tuning,<sup>101–103</sup> Koopmans’ theorem is used as the basis to derive the range-separation parameters, such that the energy of the HOMO of a molecule matches its ionisation potential (IP) calculated as the energy difference between the  $N$  and  $N - 1$  electron systems, where  $N$  is the total number of electrons in the molecule.

Körzdörfer and co-workers have carried out a series of works looking at the effect of using IP-tuned functionals on  $G_0W_0$ , and concluded that the tuning procedure leads to an improvement in the performance of DFT and  $G_0W_0$  with respect to the computation of vertical IPs and electron affinities.<sup>61,104,105</sup> As a result, we also tested the use of the IP-tuned LC- $\omega$ PBE\* functional to calculate vibronic coupling constants. Further details about the IP-tuning process in this work are given in the Supplementary Material S1 C.

Finally, the  $G_0W_0$  correction was applied on top of these functionals, and the gradients of the quasiparticle energies corresponding to the energies of the degenerate HOMOs used to calculate the orbital vibronic coupling constants. The RI-cc-pVTZ basis set<sup>106</sup> was used in the resolution of identity approach to the random phase approximation in the  $G_0W_0$  calculations.<sup>107</sup> All basis sets were taken from the Basis Set Exchange.<sup>108</sup> Additional details regarding the CP2K parameters used to ensure the numerical convergence of our results are given in the Supplementary Material S1 D.

## IV. RESULTS AND DISCUSSION

### A. Ionisation potential of the cyclopentadienyl anion

We start our discussion of the results by looking at the IP of the cyclopentadienyl anion calculated using the DFT orbital energies and  $G_0W_0$  quasiparticle energies (Table II). A number of studies<sup>62,63,65,107,110</sup> have found a strong dependence of the  $G_0W_0$  quasiparticle energies on the basis set, hence we also calculated the IPs using the cc-pVDZ and cc-pVQZ basis sets.<sup>91</sup> Our findings regarding the basis set effect is largely in agreement with the findings of these earlier studies. The cc-pVDZ basis set is clearly insufficient for the calculation of ionisation energies, with differences of about 0.4 eV to the largest cc-pVQZ basis set for HF and DFT, while the respective differences for  $G_0W_0$  are even higher at about 0.8 eV. The difference between the  $G_0W_0$  IPs calculated with the cc-pVTZ and cc-pVQZ basis sets were found to be a lot smaller in comparison, with differences for the HF and

TABLE II. Negative  $G_0W_0$  quasiparticle energies (eV) of  $\psi_\theta$ . The negative orbital energies of the method used as the input for the  $G_0W_0$  calculations is given in parentheses. Experiment:  $1.808 \pm 0.006$ ,<sup>34</sup> CCSDT/CBS: 1.785/1.816 for the two separate JT distorted geometries<sup>109</sup>

	$G_0W_0@HF$	$G_0W_0@PBE$	$G_0W_0@PBE0$	$G_0W_0@LC-\omega PBE$	$G_0W_0@LC-\omega PBE^*$
cc-pVDZ	1.441(1.515)	0.788(-1.561)	0.998(-0.517)	1.152(2.068)	1.128(1.472)
cc-pVTZ	1.951(1.714)	1.391(-1.219)	1.573(-0.232)	1.729(2.310)	1.721(1.754)
cc-pVQZ	2.200(1.825)	1.631(-1.066)	1.817(-0.100)	1.975(2.412)	1.976(1.874)

DFT values lying slightly above 0.1 eV on average, and about 0.2 eV for the corresponding  $G_0W_0$  differences.

We will thus use the results obtained using the largest cc-pVQZ basis set for the rest of this part of the discussion. The experimental IP of the cyclopentadienyl anion has been measured to be 1.808 eV using photoelectron spectroscopy,<sup>34</sup> which agrees well with the computational value of 1.785/1.816 eV at the CCSDT/CBS level of theory.<sup>109</sup> In this work, although the accuracy of the IPs computed using DFT and HF were found to vary extensively, with the exception of  $G_0W_0@HF$ , the results after applying the  $G_0W_0$  correction were found to lie within 0.2 eV of the literature values. We thus conclude that the IPs calculated within  $G_0W_0$  were found to be in good agreement with the literature.

The utility of the  $G_0W_0$  correction to DFT can be further seen from the  $G_0W_0@PBE$  and  $G_0W_0@PBE0$  results. The PBE and PBE0 functionals were found to give physically inaccurate negative values for the IP (PBE: -1.066 eV, PBE0: -0.100 eV), which can be explained by the inability of these functionals to properly account for the self-interaction or delocalisation error in DFT.<sup>111–114</sup> The application of the  $G_0W_0$  correction to PBE and PBE0 then gives rise to a substantial improvement in the computed values, with positive IPs calculated for both the  $G_0W_0@PBE$  (1.631 eV) and  $G_0W_0@PBE0$  (1.817 eV) values, and an excellent agreement between the  $G_0W_0@PBE0$  result and the literature values on top of that.

The overestimation of the IP calculated with LC- $\omega$ PBE is also reduced from 2.412 eV to 1.975 eV with the use of  $G_0W_0$ , but the  $G_0W_0@HF$  result is worsened compared to its initial value. We note that the initial HF value was found to match the literature value closely, which suggests that there could be some error cancellation between the lack of electron correlation and the use of an incomplete basis set. The application of the  $G_0W_0$  correction then improves upon the treatment of electron correlation, which results in the reduction of this error cancellation, and thus a more inaccurate IP for  $G_0W_0@HF$  as compared to the initial HF result.

A final point to note is the superior accuracy of the IP computed using the LC- $\omega$ PBE\* functional compared to the original LC- $\omega$ PBE functional. The IP calculated within LC- $\omega$ PBE (2.412 eV) severely overestimates the literature value, but the accuracy of the IP is considerably improved upon IP-tuning in LC- $\omega$ PBE\* (1.874 eV), which is in excellent agreement with the literature. The superior performance of cc-pVTZ over cc-pVQZ for the

IP-tuned LC- $\omega$ PBE\* functional can be explained by the difference between the basis sets used in the tuning of the range-separation parameter (cc-pVTZ) and the calculation of the IPs.

On the whole, we can conclude that the use of the  $G_0W_0$  correction does indeed return more accurate IPs compared to the initial HF or DFT calculations. As discussed in Section II A, the computed orbital or quasiparticle energies are linked to the calculation of vibronic coupling constants. In the following subsection, we then examine if this improvement in the computed IPs computed using the orbitals of the cyclopentadienyl anion results in a corresponding improvement in the derived vibronic coupling constants of the cyclopentadienyl radical.

## B. Linear vibronic coupling constants

First, although the  $G_0W_0$  quasiparticle energies were observed to be strongly dependent on the basis set (Section IV A), the basis set effect on the calculation of the linear vibronic coupling constants was found to be significantly weaker in comparison (Supplementary Material S2 A). This can be rationalised by considering the method of determining the linear vibronic coupling constants, which is reliant on the gradients of the orbital or quasiparticle energies instead of their absolute values. As the energy gradients are determined numerically with respect to the distortion of the parent cyclopentadienyl anion, there is likely to be some cancellation in the basis set errors, thus reducing the dependence of the calculated vibronic coupling constants on the basis set. We thus used the cc-pVTZ basis set for the rest of this work.

The present results for the computed linear vibronic coupling constants are given in Tables III and V. We first note that our results satisfy the Wigner-Eckart theorem, with the magnitudes of the linear coupling constants calculated using the  $e'_2(\theta)$  or  $e'_2(\epsilon)$  normal modes and the gradients of the energies of  $\psi_\theta$  and  $\psi_\epsilon$  effectively equal throughout (Supplementary Material S2 B). As per earlier work,<sup>22,30,34,74</sup> the vibronic coupling constants of  $\nu_{12}$  (C–H stretching) was found to be a lot smaller than the other three  $e'_2$  normal modes, and should not contribute significantly to the JT distortion in the cyclopentadienyl radical. Our discussion of the vibronic coupling constants obtained using the different exchange-correlation functionals and  $G_0W_0$  will thus focus on the other three  $e'_2$  normal modes:  $\nu_9$ ,

TABLE III. Linear vibronic coupling constants of the  $e'_2(\theta)$  normal modes calculated using the gradients of the  $G_0W_0$  quasiparticle energies for  $\psi_\theta$ : (orbital) vibronic coupling constant  $V^{(1)}$  ( $10^{-4}$  a.u.), dimensionless vibronic coupling constant  $g^{(1)} = V^{(1)}/\sqrt{\hbar\omega^3}$ , and the JT stabilisation energy  $E_{JT}^{(1)} = (1/2)(V^{(1)}/\omega)^2$  ( $\text{cm}^{-1}$ ).  $\omega$  ( $\text{cm}^{-1}$ ) is the second order derivative of the total HF/DFT energies of the cyclopentadienyl anion along the PBE0/cc-pVTZ vibrational eigenmodes, and are taken to be the harmonic frequencies within the respective methods. The corresponding values obtained with the mean-field DFT/HF method used as the input to the  $G_0W_0$  calculations are given in parentheses, while the results obtained using  $\psi_\epsilon$  is given in the Supplementary Material S2B

Mode		$G_0W_0@$ HF	$G_0W_0@$ PBE	$G_0W_0@$ PBE0	$G_0W_0@$ LC- $\omega$ PBE	$G_0W_0@$ LC- $\omega$ PBE*	Expt. <sup>a</sup>	CASSCF <sup>b</sup>	CASSCF <sup>c</sup>	EOMIP- CCSD <sup>d</sup>
$\nu_9$	$\omega$	915	816	844	854	835	872[830]	817	914	834
	$V^{(1)}$	1.75(1.90)	1.59(1.62)	1.65(1.68)	1.69(1.61)	1.67(1.56)	1.54[1.68]	1.76	2.12	1.42
	$g^{(1)}$	0.651(0.705)	0.701(0.715)	0.691(0.702)	0.695(0.661)	0.710(0.666)	0.66[0.72]	0.77	0.79	0.60
	$E_{JT}^{(1)}$	194(227)	201(208)	202(208)	206(187)	211(185)	166[216]	245	285	153
$\nu_{10}$	$\omega$	1146	1030	1061	1066	1044	1041[1058]	1061	1144	1063
	$V^{(1)}$	2.98(3.14)	2.64(2.53)	2.77(2.72)	2.92(2.94)	2.87(2.76)	3.49[2.41]	3.29	4.89	2.94
	$g^{(1)}$	0.791(0.834)	0.823(0.786)	0.825(0.810)	0.862(0.870)	0.874(0.842)	1.07[0.72]	0.98	1.30	0.87
	$E_{JT}^{(1)}$	358(398)	349(318)	361(348)	396(404)	398(370)	594[275]	509	977	404
$\nu_{11}$	$\omega$	1446	1395	1410	1422	1413	1320[1410]	1415	1497	1434
	$V^{(1)}$	6.68(7.34)	5.51(5.04)	5.89(5.69)	6.32(6.61)	6.15(5.97)	3.96[6.01]	7.25	5.97	6.31
	$g^{(1)}$	1.25(1.37)	1.09(0.994)	1.14(1.10)	1.21(1.27)	1.19(1.16)	0.85[1.17]	1.40	1.06	1.20
	$E_{JT}^{(1)}$	1128(1362)	825(690)	921(860)	1044(1141)	1002(944)	477[959]	1387	841	1025
$\nu_{12}$	$\omega$	3239	3189	3139	3235	3214		3040	3263	3169
	$V^{(1)}$	-0.136(0.043)	0.329(0.260)	0.289(0.200)	0.270(0.058)	0.297(0.117)			1.45	0.24
	$g^{(1)}$	-0.008(0.002)	0.019(0.015)	0.017(0.012)	0.015(0.003)	0.017(0.007)			0.08	0.01
	$E_{JT}^{(1)}$	<1(<1)	<1(<1)	<1(<1)	<1(<1)	<1(<1)		<1	10	<1

<sup>a</sup> Reference 74. The values obtained using an alternative fit to the measured spectra are given in brackets (see text).

<sup>b</sup> Scaled CAS(5, 5) results. Method I in Reference 30. Frequencies were calculated within generalised restricted HF in this work, and scaled by 0.89.

<sup>c</sup> Scaled CAS(5, 8) results in Reference 22. Frequencies  $\omega$  were calculated within restricted HF in this work.

<sup>d</sup> Reference 34, effectively identical to the EOMIP-CCSD values in reference 75.

$\nu_{10}$ , and  $\nu_{11}$ .

TABLE IV. Comparison of the standard deviation in the linear vibronic coupling constant  $V^{(1)}$  ( $10^{-4}$  a.u.) calculated using the mean-field HF/DFT methods, and  $G_0W_0$ .

	Mean-field methods	$G_0W_0$
$\nu_9$	0.132	0.059
$\nu_{10}$	0.235	0.132
$\nu_{11}$	0.881	0.442

In contrast to the computed IP of the cyclopentadienyl anion discussed earlier in Section IV A, the effect of the exchange-correlation functional was found to be small, with the magnitude of the vibronic coupling constants of the individual normal modes roughly following the order: PBE < PBE0, LC- $\omega$ PBE\* < LC- $\omega$ PBE < HF. Thus, unlike the IPs discussed in the preceding subsection, there does not appear to be any clear benefit in the use of an IP-tuned functional for the linear vibronic coupling constant. The HF values of  $V^{(1)}$  and  $\omega$  were clearly larger than those calculated with DFT, but the corresponding difference between the values for  $g^{(1)}$  and  $E^{(1)}$  is slightly reduced by the larger HF values of  $V^{(1)}$  and  $\omega$  cancelling each other out. This follows the observed weakening of the basis set effect earlier, which again suggests that the protocol used to derive the vibronic coupling constants in this work appears to be relatively independent of the exact computational method used.

We then examine the linear vibronic coupling constants calculated with  $G_0W_0$ .  $G_0W_0$  is the first order perturbative correction to a HF or DFT calculation, and the inclusion of additional correction terms should eventually converge the results towards a self-consistent  $GW$  value (Section II B). Thus, although our  $G_0W_0$  results show a similar dependence on the starting point as that observed in earlier studies,<sup>61,62,65</sup> the difference between the  $G_0W_0$  results is smaller compared to that of the DFT and HF values. As can be seen in Table IV, the standard deviation in the  $G_0W_0$  computed values of  $V^{(1)}$  is about half the standard deviation for the HF and DFT results. This clearly shows a benefit in the use of  $G_0W_0$ : the dependence of the choice of exchange-correlation functional is reduced.

Next, we compare the linear vibronic coupling constants derived in this work to the literature (Table III). The computational and experimental data for  $\nu_9$  in the literature is generally in agreement with each other, with Sato's CASSCF calculations giving slightly

higher values. Our DFT and  $G_0W_0$  results for  $\nu_9$  also agrees well with the literature, while the higher HF values was alleviated by the  $G_0W_0$  correction.

However, there is some uncertainty in the literature regarding the relative strengths of the vibronic coupling in  $\nu_{10}$  and  $\nu_{11}$ . The fitting of the dispersed fluorescence spectra measured by Applegate *et al.*<sup>74</sup> gave a larger vibronic coupling constant for  $\nu_{10}$  than  $\nu_{11}$ , which disagrees with their own CASSCF calculations.<sup>30</sup> The EOMIP-CCSD results of Ichino *et al.*<sup>34</sup> agree with the CASSCF results of Applegate *et al.*, while the observed trend by Sato *et al.*<sup>22</sup> follows the experimental result more closely.

To resolve this, we note that there has been some ambiguity regarding the assignments of the vibronic peaks in the dispersed fluorescence spectra.<sup>74</sup> An alternative fit to the measured spectra “had a slightly worse RMS [root-mean-square] error of  $6.3 \text{ cm}^{-1}$ , but is in better agreement with the constants derived from *ab initio* calculations.”<sup>74</sup> The values for the vibronic coupling constants of  $\nu_9$  remain mostly unchanged if the alternate fit is used, while the corresponding values for  $\nu_{10}$  and  $\nu_{11}$  decreases and increases respectively (Table III). In addition, the photoelectron spectrum of the cyclopentadienyl anion was simulated using the vibronic coupling constants calculated within EOMIP-CCSD, and was found to reproduce the experimentally measured photoelectron spectrum well.<sup>34</sup> On the other hand, the use of the vibronic coupling constants obtained with the original fit of the dispersed fluorescence spectra to carry out a similar simulation “worsens the quality of the simulation significantly”. Indeed, a recent paper by Tran *et al.* showed that a low RMS error in the fitting of a spectrum is not necessarily correlated with a small error in the values of the vibronic coupling constants obtained from the fit,<sup>33</sup> and further emphasises the uncertainty in the vibronic assignment of the dispersed fluorescence spectra.

Because of these issues with the experimental result, we do not compare our results for  $\nu_{10}$  and  $\nu_{11}$  to experiment, and will use the computational values as a benchmark instead. On the whole, the HF and DFT results were found to agree quite well with the computational values in the literature, with none of the methods tested found to outperform the others substantially. The PBE, PBE0 and LC- $\omega$ PBE\* functionals underestimate the reference CASSCF and EOMIP-CCSD values, while the results for HF and LC- $\omega$ PBE are mixed, depending on which vibronic constant is being compared. These trends for the individual functionals and HF are balanced out upon applying the  $G_0W_0$  correction, and we note that there is an excellent agreement between our  $G_0W_0$  results and the EOMIP-CCSD

calculations of Ichino *et al.*.

In the EOMIP-CCSD method, the electronic state of the (open-shell) system is described by determinants with one less electron than the reference state, which is typically chosen to be a closed-shell system.<sup>115</sup> This allows for a balanced treatment of the determinants representing the electronic configurations of the  $N - 1$  electron system, where  $N$  is the number of electrons in the reference state.<sup>116</sup> As a result, EOMIP-CCSD “can handle multireference effects while dynamic electron correlation is also taken into account”,<sup>35,117</sup> making it a suitable computational method to study the neutral cyclopentadienyl radical directly.

In contrast, because we used the orbitals of the cyclopentadienyl anion to study the JT effect of the neutral cyclopentadienyl radical, it would not be necessary to consider the problem of static electron correlation in our work. The  $G_0W_0$  approximation was then used to improve upon the treatment of dynamic electron correlation. Comparing the computational costs of the two methods, EOMIP-CCSD and  $G_0W_0$  scale on the order of  $\mathcal{O}(N^6)$  and  $\mathcal{O}(N^4)$  respectively.<sup>107,115</sup> Hence, despite the difference between the two approaches, the fact that the  $G_0W_0$  results in this work were found to be of EOMIP-CCSD quality is definitely noteworthy, and supports the usage of  $G_0W_0$  in the derivation of vibronic coupling constants.

We then examine the total JT stabilisation energies for the last part of the discussion regarding the linear vibronic coupling constants (Table V). There are two approaches used to obtain the total stabilisation energies in the literature. The first approach, which is used in this work, fits *ab initio* data to a model vibronic Hamiltonian to extract the vibronic coupling constants for each JT active normal mode, before summing up the individual stabilisation energies for each normal mode to obtain the total stabilisation energy. The second approach compares the difference in the energies of the cyclopentadienyl radical at the  $D_{5h}$  and  $C_{2v}$  optimised geometries.

A point to note is that some vibronic coupling studies use a combination of the two methods to derive the vibronic coupling constants. Vibronic coupling constants are initially obtained by fitting to *ab initio* results to a model Hamiltonian, before being scaled such that the calculated energies matches the stabilisation energies computed in the second approach.<sup>22,30</sup> This is a possible explanation to the difference in the observed trends between the computational results of Sato *et al.* and the present work.

The stabilisation energies obtained using the first method generally agree well with each other as well as the experimental value obtained using the alternate fit of the dispersed

TABLE V. Linear JT stabilisation energies  $E_{JT}^{(1)}$  ( $\text{cm}^{-1}$ ) calculated within  $G_0W_0$ . The values for the mean-field method used as an input in the  $G_0W_0$  calculations is given in parentheses.

Method	$E_{total}^{(1)}$
$G_0W_0@HF/cc-pVTZ$	1680(1988)
$G_0W_0@PBE/cc-pVTZ$	1374(1217)
$G_0W_0@PBE0/cc-pVTZ$	1484(1417)
$G_0W_0@LC-\omega PBE/cc-pVTZ$	1647(1732)
$G_0W_0@LC-\omega PBE^*/cc-pVTZ$	1612(1499)
Model potential <sup>a</sup>	
EOMIP-CCSD/DZP <sup>34</sup>	1510
EOMIP-CCSD/ANO0 <sup>75</sup>	1600
CASSCF/6-31G* <sup>30</sup>	1463
Energy difference <sup>b</sup>	
CCSDT/CBS <sup>109</sup>	1370
CCSD(T)/6-311+G* <sup>78</sup>	1600
CASSCF/6-31G* <sup>30</sup>	2147
CASSCF/cc-pVDZ <sup>32</sup>	2134
CASSCF/6-31G(d, p) <sup>22</sup>	2103
LDA/TZP <sup>15</sup>	1245
BP86/TZP <sup>15</sup>	1302
PW91/TZP <sup>15</sup>	1295
BLYP/TZP <sup>15</sup>	1303
OPBE/TZP <sup>15</sup>	1300
B3LYP/TZP <sup>15</sup>	1686
Expt. <sup>74</sup>	1237[1600] <sup>c</sup>

<sup>a</sup> Sum of the stabilisation energies over all linear JT active normal modes

<sup>b</sup> Difference in the energies of the cyclopentadienyl radical at the  $D_{5h}$  and  $C_{2v}$  geometries

<sup>c</sup> In brackets: stabilisation energy from an alternate fit of the dispersed fluorescence spectra (see text)

fluorescence spectra. On the other hand, the stabilisation energies calculated using the second method was found to vary widely. The CCSDT and CCSD(T) stabilisation energies ( $1370 \text{ cm}^{-1}$  and  $1600 \text{ cm}^{-1}$  respectively) are lower than the CASSCF values, which are all greater than  $2100 \text{ cm}^{-1}$ . The DFT stabilisation energies of Andjelković *et al.*<sup>15</sup> are in better agreement with the lower CCSDT and CCSD(T) values, and exhibits a clear dependence

on the amount of HF exchange in the functional used, matching the trend observed in our own DFT results. On the whole, the stabilisation energies calculated using CASSCF with the second method appears to be an overestimation. We suggest that this could be due to dynamic correlation, which is not accounted for in the CASSCF method,<sup>41,42</sup> but is accounted for in the CCSDT and CCSD(T) methods.<sup>118–120</sup>

As mentioned above, the DFT and HF stabilisation energies calculated in this work is largely dependent on the amount of HF exchange present, and follows the order: PBE < PBE0 < LC- $\omega$ PBE < LC- $\omega$ PBE\* < HF. The difference between the total stabilisation energies calculated using the various computational methods comes mostly from  $\nu_{11}$ , while the differences for  $\nu_9$  and  $\nu_{10}$  are much smaller. A comparison of the the LC- $\omega$ PBE to LC- $\omega$ PBE\* results suggests that there is a slight improvement in the calculated stabilisation energies upon IP-tuning. Similar to the other vibronic coupling constants, the spread of the calculated DFT and HF values is reduced upon applying the  $G_0W_0$  correction. The total stabilisation energies for HF and LC- $\omega$ PBE is decreased, while the values for the other functionals are increased. The resultant  $G_0W_0$  stabilisation energies are again in good agreement with the EOMIP-CCSD values, and exemplifies the potential of the  $G_0W_0$  method.

Hence, to sum up the discussion of the linear vibronic coupling constants, the choice of the exchange-correlation functional was not found to affect the derived vibronic coupling constants of each normal mode significantly. Regardless of the starting point, the use of the  $G_0W_0$  correction was found to improve upon the HF and DFT results, and yielded results of EOMIP-CCSD quality.

Finally, despite the good agreement between our results for the linear vibronic coupling constants and those in the literature, some studies have shown that the inclusion of higher order vibronic terms in the model Hamiltonian can affect the values of the fitted vibronic coupling constants.<sup>33,37</sup> Other than their effect on the fitting of linear vibronic coupling constants, the inclusion of higher order vibronic coupling terms in the vibronic model potential of a system also affects its APES directly.<sup>20,27,33,36–38</sup> As a result, we extend our vibronic Hamiltonian to go beyond the consideration of only linear vibronic coupling, and examine the use of a higher order Hamiltonian to fit our *ab initio* data in the next subsection.

### C. Higher order vibronic coupling terms

The details of the derivation and fitting of the higher order vibronic Hamiltonians are given in the Appendix, and the results are given in Table VI and the Supplementary Material S2C. Since we only consider symmetrized combinations of the  $e'_2$  normal modes in this work, the quadratic vibronic Hamiltonian in this subsection is equivalent to the linear JT model discussed in the previous section. As per the previous section, we do not include  $\nu_{12}$  in the discussion because it does not make a significant contribution to the JT distortion in the cyclopentadienyl radical.

We will illustrate our findings for the higher order vibronic coupling terms by considering the results obtained using PBE0 (Table VI). There is a general consensus in the literature that there is no pseudorotation barrier in the cyclopentadienyl radical.<sup>29–32,34,77,82,83,109</sup> The only exception is a pseudorotation barrier height of about  $300\text{ cm}^{-1}$  predicted within CISD,<sup>29,77</sup> which has been “attributed to an artificial effect caused by the CISD computation.”<sup>77</sup>

Our results agree well with the reported trend in the general literature. It can be seen from Table IX in the Appendix that only the fourth order  $V_{e'_2}^{(4)}$  term gives rise to a pseudorotation barrier in the cyclopentadienyl radical. However, the magnitude of the contribution to the JT stabilisation energy by the fourth order vibronic coupling constants at  $\rho_{min.}$  were all found to be  $< 1\text{ cm}^{-1}$  for each of the  $e'_2$  normal modes  $\nu_9$ ,  $\nu_{10}$  and  $\nu_{11}$ . As such, we find that there is effectively no pseudorotation barrier in the cyclopentadienyl radical.

In addition, the same analysis of the third order vibronic coupling term revealed a similar insignificance in terms of its contribution to the JT stabilisation energy. As can be seen from Figure 5, we find that the APES determined using the second, third, and fourth order model vibronic Hamiltonian are essentially identical in the case of the cyclopentadienyl radical.

The same trends were observed for HF and the other exchange-correlation functionals, as well as  $G_0W_0$  (Supplementary Material S2C). It is thus clear that any JT distortion originating from the  $e'_2$  normal modes will be largely dominated by the linear vibronic coupling term,  $V_{e'_2}^{(1)}$ , which has been discussed in the preceding section. Hence, we do not find it meaningful to examine the differences between the higher order vibronic coupling terms derived using HF, the various DFT functionals and  $G_0W_0$ .

Finally, we examine the effect of using a higher order vibronic Hamiltonian on the derived vibronic coupling constants. As expected, the RMS of the fitting error to the orbital energies

TABLE VI. Higher order vibronic coupling constants derived using PBE0.  $V_\gamma^{(i)}$  refers to the  $i^{\text{th}}$  order vibronic coupling constant with respect to the symmetry representation  $\gamma$ ,  $\rho_{min}$  refers to the molecular structure at which the energy of the system is at a minima with respect to the distortion along a  $e'_2$  normal mode, and  $E_{JT}^{(i)}$  refers to the JT stabilisation energy, where  $i$  is the order of the model Hamiltonian used. All values are in a.u. except for the stabilisation energies, which is given in  $\text{cm}^{-1}$

Mode	Order	$V_{e'_2}^{(1)} \times 10^{-4}$	$V_{a'_1}^{(2)} \times 10^{-5}$	$V_{e'_2}^{(3)} \times 10^{-9}$	$V_{e'_2}^{(4)} \times 10^{-10}$	$V_{a'_1}^{(4)} \times 10^{-9}$	$\rho_{min.}$	$E_{JT}^{(i)}$ <sup>a</sup>
$\nu_9(\theta)$	2	1.6756	2.0953				11.309	207.94
	3	1.6753	2.0953	1.4622			11.310	207.90
	4	1.6753	2.0950	1.4622	0.3349	1.6215	11.304	207.96
$\nu_9(\epsilon)$	2	1.6763	2.0953				11.314	208.11
	3	1.6760	2.0953	1.4430			11.315	208.08
	4	1.6760	2.0950	1.4430		1.6175	11.309	208.14
$\nu_{10}(\theta)$	2	2.7214	3.3298				11.558	345.18
	3	2.7205	3.3298	4.6618			11.561	345.08
	4	2.7205	3.3040	4.6618	0.0355	17.8736	11.514	345.69
$\nu_{10}(\epsilon)$	2	2.7221	3.3298				11.561	345.35
	3	2.7212	3.3298	4.5872			11.564	345.24
	4	2.7212	3.3040	4.5872		17.8856	11.516	345.86
$\nu_{11}(\theta)$	2	5.6879	5.8738				13.695	854.79
	3	5.6898	5.8738	-9.1704			13.689	854.92
	4	5.6898	5.8398	-9.1704	15.7283	23.5324	13.589	854.20
$\nu_{11}(\epsilon)$	2	5.6874	5.8738				13.693	854.63
	3	5.6892	5.8738	-9.0769			13.688	854.76
	4	5.6892	5.8398	-9.0769		23.5420	13.598	854.39

<sup>a</sup> The value of  $E_{JT}^{(2)}$  differs slightly from  $E_{JT}^{(1)}$  in Table III because the PBE0 analytical frequencies were used in the calculation of  $E_{JT}^{(1)}$  earlier, while the fitted second order derivative of the SCF energies was used to compute  $E_{JT}^{(2)}$  here in order to compare the differences between the higher order vibronic Hamiltonians.

decreases with respect to the order of the vibronic Hamiltonian used to fit the *ab initio* data (Table VII). However, we note that the RMS errors of the smallest second order model are already about two to three orders of magnitude smaller than the derived linear vibronic

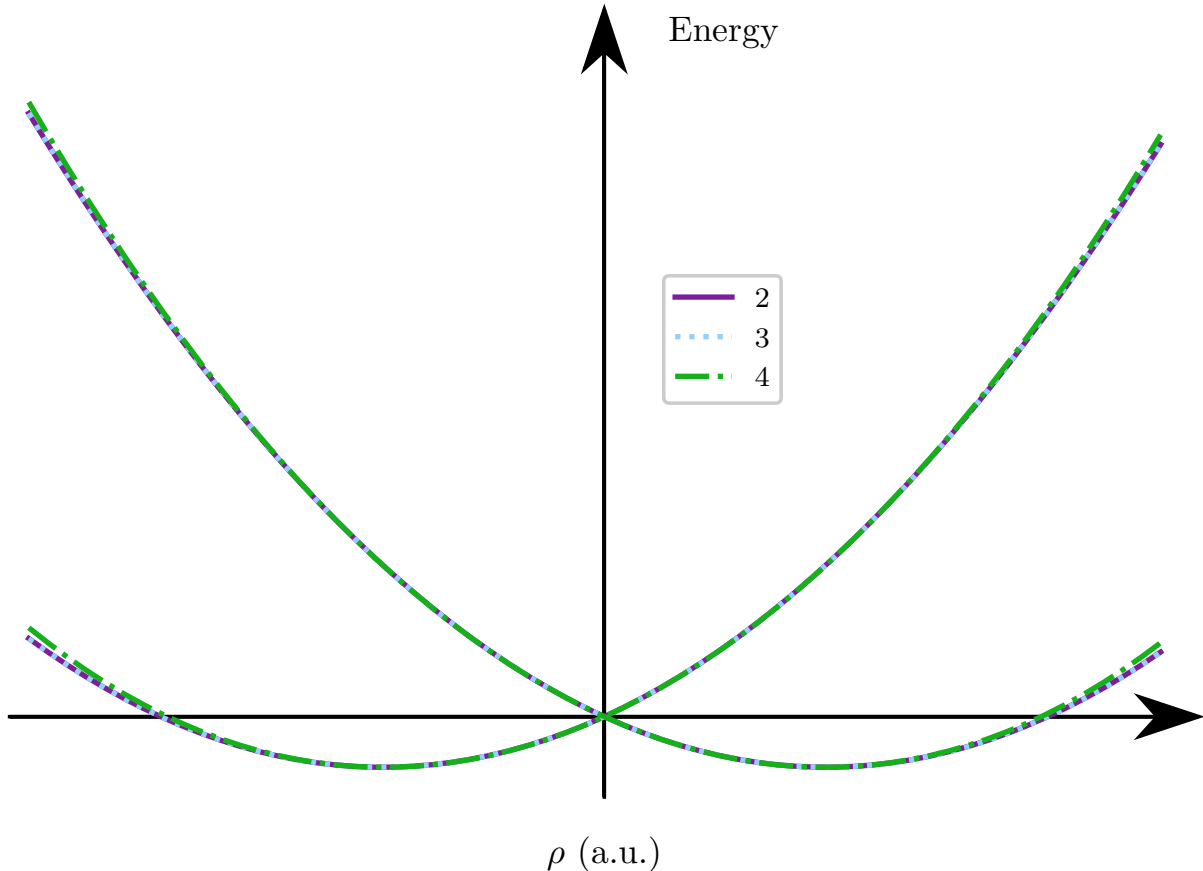


FIG. 5. APES of the cyclopentadienyl radical calculated using a quadratic, cubic, and quartic vibronic Hamiltonian. The vibronic coupling constants were determined using PBE0 (Table VI).

coupling constants, which implies that the quality of the quadratic fit is already excellent. As such, the linear vibronic coupling constant were found to remain virtually unchanged going from the quadratic to the quartic model Hamiltonian (Table VI). Considering that the JT distortion in the cyclopentadienyl radical is essentially due to linear vibronic coupling only, it is thus not surprising that the effect of using a higher order vibronic model was not found to affect the derived vibronic coupling constants significantly.

To conclude the discussion of using a higher order vibronic Hamiltonian, we agree with the conclusions in Tran *et al*'s work: a low RMS error of the fitted model does not necessarily correlate with the quality of the derived vibronic coupling constants.<sup>33</sup> However, because the higher order vibronic coupling of the  $e'_2$  normal modes is very weak compared to the linear vibronic coupling terms, the effect of including higher order  $e'_2$  terms in the model vibronic Hamiltonian cannot be clearly observed in this case. Hence, we did not observe any change

TABLE VII. RMS error ( $10^{-8}$  a.u.) of the fit to the PBE0 orbital energy corresponding to the  $E_1''(\theta)$  electronic state.

Mode	Order of vibronic model		
	Quadratic	Cubic	Quartic
$\nu_9(\theta)$	14.79	0.88	0.83
$\nu_9(\epsilon)$	14.70	1.87	1.66
$\nu_{10}(\theta)$	47.94	12.58	1.69
$\nu_{10}(\epsilon)$	48.56	12.51	0.84
$\nu_{11}(\theta)$	98.30	32.29	1.74
$\nu_{11}(\epsilon)$	91.26	3.70	1.25

in the values of the linear vibronic coupling constants upon the use of a higher order vibronic Hamiltonian to fit *ab initio* calculations. As such, we find it sufficient to include only the first order terms of the linear JT active  $e_2'$  normal modes to describe the JT distortion, and by extension, the APES of the cyclopentadienyl radical.

Finally, we did not include normal modes that are not linear JT active, such as the  $e_1'$  normal modes in the cyclopentadienyl radical, within our model of vibronic coupling. The higher order vibronic coupling terms of some of these normal modes are symmetry-allowed, which suggests they could contribute to the JT distortion in the cyclopentadienyl radical. Hence, possible future work to examine the effect of higher order vibronic coupling terms could be to consider normal modes that are not linear JT active, such as the  $e_1'$  normal modes in the cyclopentadienyl radical, in the vibronic model of the system of interest as well.

## V. CONCLUSION

The use of HF, DFT with various exchange-correlation functionals and  $G_0W_0$  to derive the vibronic coupling constants of the cyclopentadienyl radical has been investigated in this work. Towards that end, the IP of the cyclopentadienyl anion was first calculated, and a

notable improvement to the HF and DFT values upon applying the  $G_0W_0$  correction was found.

Next, the linear vibronic coupling constants were calculated from the gradients of the degenerate HOMOs of the cyclopentadienyl anion for HF and DFT, with the gradients of the corresponding quasiparticle energies used for  $G_0W_0$ . However, unlike the results for the IP, the choice of the specific computational method (HF or the various DFT functionals) was not found to have a significant effect on the obtained linear vibronic coupling constants. Applying the  $G_0W_0$  correction then further reduces the differences between the linear vibronic coupling constants derived using the various computational methods, and were found to yield values that agree well with EOMIP-CCSD values from the literature.

Finally, the vibronic coupling model was expanded to include higher order vibronic coupling terms up to the fourth order. The higher order vibronic coupling constants in the cyclopentadienyl radical were found to be negligible in comparison to the linear vibronic coupling constants. Consequently, our results show that there is effectively no pseudorotation barrier in the cyclopentadienyl radical, in good agreement with what has been observed in the literature.

In sum, we have shown that the JT effect in the cyclopentadienyl radical can be well understood by considering only the linear vibronic coupling terms, which can be derived accurately with the use of  $G_0W_0$ . As such, we can thus conclude that computational approaches that rely on Hedin’s approximations, such as the  $G_0W_0$  method examined in this work, have the potential to be an excellent tool towards studying vibronic coupling, and thus the APES of molecular systems.

## **SUPPLEMENTARY ONLINE MATERIAL**

See Supplementary Material for additional details regarding the factors affecting the fitting process, the numerical convergence of our computational results, and the IP-tuning procedure used to obtain the range-separation parameter of the LC- $\omega$ PBE\* functional. The derived vibronic coupling constants and plots of the orbital and quasiparticle energies obtained with the various exchange-correlation functionals and  $G_0W_0$  are also included.

## DATA AVAILABILITY

The data that supports the findings of this study are available within the article and its supplementary material.

## ACKNOWLEDGMENTS

We thank Dr. Naoya Iwahara for suggesting this study and for useful discussions during its implementation. Scientific grants R-143-000-A80-114, R-143-000-A65-133 from the Ministry of Education, Singapore are gratefully acknowledged. Computational resources from the National Supercomputing Centre (ASPIRE-1, grant 11001278) and the High Performance Computing services at the National University of Singapore (NUS) Computer Centre were used for this study.

## Appendix: Higher order vibronic coupling terms

The details of the extension of the vibronic Hamiltonian to include cubic and quartic terms is given here. The results from the same set of *ab initio* calculations were used in the derivation of the linear and higher order vibronic coupling constants. As such, we only consider the higher order vibronic coupling of the  $e'_2$  normal modes here, and ignore the inter-mode coupling across different degenerate  $e'_2$  normal modes as well.

The symmetric product of the  $e'_2$  representation up to the fourth order is given in Table VIII. As per Equation 10, only the terms with  $a'_1$  and  $e'_2$  symmetry will be JT active. The contribution of each  $e'_2$  normal mode to  $\Delta U$  in Equation 6 can then be grouped into

TABLE VIII. Symmetric products of the  $e'_2$  representation up to the fourth order

Order	Product
1	$e'_2$
2	$e'_2 \otimes e'_2 = a'_1 \oplus e'_1$
3	$e'_2 \otimes e'_2 \otimes e'_2 = e'_1 \oplus e'_2$
4	$e'_2 \otimes e'_2 \otimes e'_2 \otimes e'_2 = a'_1 \oplus e'_1 \oplus e'_2$

symmetrized combinations of the  $e'_2$  normal coordinates,  $Q_\theta$  and  $Q_\epsilon$ , up to the fourth order as

$$\begin{aligned}
\Delta U(Q_\theta, Q_\epsilon) = & V_{e'_2(\theta)}^{(1)} Q_\theta + V_{e'_2(\epsilon)}^{(1)} Q_\epsilon + \frac{V_{a'_1}^{(2)}}{2!} \left[ \frac{1}{\sqrt{2}} (Q_\theta^2 + Q_\epsilon^2) \right] \\
& + \frac{V_{e'_2(\theta)}^{(3)}}{3!} \left[ \frac{1}{2} (Q_\theta^3 + Q_\theta Q_\epsilon^2) \right] + \frac{V_{e'_2(\epsilon)}^{(3)}}{3!} \left[ \frac{1}{2} (Q_\epsilon^3 + Q_\epsilon Q_\theta^2) \right] \\
& + \frac{V_{e'_2(\theta)}^{(4)}}{4!} \left[ \frac{1}{2\sqrt{2}} (Q_\theta^4 - 6Q_\theta^2 Q_\epsilon^2 + Q_\epsilon^4) \right] + \frac{V_{e'_2(\epsilon)}^{(4)}}{4!} \left[ \frac{-4}{2\sqrt{2}} (Q_\theta^3 Q_\epsilon - Q_\theta Q_\epsilon^3) \right] \\
& + \frac{V_{a'_1}^{(4)}}{4!} \left[ \frac{1}{2\sqrt{2}} (Q_\theta^4 + 2Q_\theta^2 Q_\epsilon^2 + Q_\epsilon^4) \right], \tag{A.1}
\end{aligned}$$

where  $V_\gamma^{(i)}$  is the  $i^{\text{th}}$  order vibronic coupling term of the symmetrized combination of  $Q_\theta$  and  $Q_\epsilon$  with the representation  $\gamma = a'_1$  or  $e'_2$ . We note that the third order  $e'_2$  term can be derived from two possible products:  $e'_2 \in e'_1 \otimes e'_2$  or  $e'_2 \in a'_1 \otimes e'_2$ . However, as the symmetrized combinations of the two possible products are identical:  $(Q_\theta^3 + Q_\theta Q_\epsilon^2)$  and  $(Q_\epsilon^3 + Q_\epsilon Q_\theta^2)$ , the two terms can be combined for simplicity. The same was done for the fourth order  $a'_1$  ( $\in e'_1 \otimes e'_1$  or  $\in a'_1 \otimes a'_1$ ) term.

Similar to the analysis of the linear JT active modes in Section II A, the Wigner-Eckart theorem is then applied to simplify the vibronic coupling matrices, *i.e.*

$$V_{e'_2}^{(i)} = V_{e'_2(\theta)}^{(i)} = V_{e'_2(\epsilon)}^{(i)} \tag{A.2}$$

for  $i = 1, 3$ , and 4. The matrix representation of the vibronic Hamiltonian up to the fourth order is then

$$\begin{aligned}
\mathbf{H}_{vib.} = & \boldsymbol{\sigma}_{e'_2(\theta)} \left[ V_{e'_2}^{(1)} Q_\theta + \frac{V_{e'_2}^{(3)}}{3!} \frac{1}{2} (Q_\theta^3 + Q_\theta Q_\epsilon^2) + \frac{V_{e'_2}^{(4)}}{4!} \frac{1}{2\sqrt{2}} (Q_\theta^4 - 6Q_\theta^2 Q_\epsilon^2 + Q_\epsilon^4) \right] \\
& + \boldsymbol{\sigma}_{e'_2(\epsilon)} \left[ V_{e'_2}^{(1)} Q_\epsilon + \frac{V_{e'_2}^{(3)}}{3!} \frac{1}{2} (Q_\epsilon^3 + Q_\epsilon Q_\theta^2) + \frac{V_{e'_2}^{(4)}}{4!} \frac{1}{2\sqrt{2}} (Q_\theta^3 Q_\epsilon - Q_\theta Q_\epsilon^3) \right] \\
& + \mathbf{I} \left[ \frac{V_{a'_1}^{(2)}}{2!} \frac{1}{\sqrt{2}} (Q_\theta^2 + Q_\epsilon^2) + \frac{V_{a'_1}^{(4)}}{4!} \frac{1}{2\sqrt{2}} (Q_\theta^4 + 2Q_\theta^2 Q_\epsilon^2 + Q_\epsilon^4) \right] \tag{A.3}
\end{aligned}$$

using the matrices

$$\boldsymbol{\sigma}_{e'_2(\theta)} = \begin{pmatrix} 1 & 0 \\ 0 & -1 \end{pmatrix}, \quad \boldsymbol{\sigma}_{e'_2(\epsilon)} = \begin{pmatrix} 0 & 1 \\ 1 & 0 \end{pmatrix}, \quad \mathbf{I} = \begin{pmatrix} 1 & 0 \\ 0 & 1 \end{pmatrix}.$$

TABLE IX. Derived expressions of the APES in terms of the polar coordinates  $\rho$  and  $\phi$ . The expressions for the second and third order models are exact, while the expression for the fourth order here is obtained by truncating Equation (A.5).

$i$	$E_{\mp}^{(i)}$
2	$\mp V'_{e_2}{}^{(1)} \rho + \frac{V'_{a_1}{}^{(2)}}{2!} \frac{\rho^2}{\sqrt{2}}$
3	$\mp V'_{e_2}{}^{(1)} \rho + \frac{V'_{a_1}{}^{(2)}}{2!} \frac{\rho^2}{\sqrt{2}} \mp \frac{V'_{e_2}{}^{(3)}}{3!} \frac{\rho^3}{2}$
4	$\mp V'_{e_2}{}^{(1)} \rho + \frac{V'_{a_1}{}^{(2)}}{2!} \frac{\rho^2}{\sqrt{2}} \mp \frac{V'_{e_2}{}^{(3)}}{3!} \frac{\rho^3}{2} \mp \frac{V'_{e_2}{}^{(4)}}{4!} \frac{\rho^4 \cos 5\phi}{2\sqrt{2}} + \frac{V'_{a_1}{}^{(4)}}{4!} \frac{\rho^4}{2\sqrt{2}}$

Diagonalising the Hamiltonian A.3 with polar coordinates  $Q_\theta = \rho \cos \phi$  and  $Q_\epsilon = \rho \sin \phi$  then gives the expression for the fourth order APES ( $E_{\mp}^{(4)}$ ) as

$$\begin{aligned}
E_{\mp}^{(4)}(\rho, \phi) &= \frac{V'_{a_1}{}^{(2)}}{2!} \frac{\rho^2}{\sqrt{2}} + \frac{V'_{a_1}{}^{(4)}}{4!} \frac{\rho^4}{2\sqrt{2}} \\
&\mp \left[ \left( V'_{e_2}{}^{(1)} \rho \right)^2 + \frac{V'_{e_2}{}^{(1)} V'_{e_2}{}^{(3)}}{3!} \rho^4 + \frac{V'_{e_2}{}^{(1)} V'_{e_2}{}^{(4)}}{4!} \frac{\rho^5 \cos 5\phi}{\sqrt{2}} \right. \\
&\quad \left. + \left( \frac{V'_{e_2}{}^{(3)}}{3!} \frac{\rho^3}{2} \right)^2 + \frac{V'_{e_2}{}^{(3)} V'_{e_2}{}^{(4)}}{3! 4!} \frac{\rho^7 \cos 5\phi}{2\sqrt{2}} + \left( \frac{V'_{e_2}{}^{(4)}}{4!} \frac{\rho^4}{2\sqrt{2}} \right)^2 \right]^{1/2}. \quad (\text{A.4})
\end{aligned}$$

Expanding the expression for the APES in Equation (A.4) as a series in  $\rho$  then gives

$$E_{\mp}^{(i)}(\rho, \phi) = \mp V'_{e_2}{}^{(1)} \rho + \frac{V'_{a_1}{}^{(2)}}{2!} \frac{\rho^2}{\sqrt{2}} \mp \frac{V'_{e_2}{}^{(3)}}{3!} \frac{\rho^3}{2} \mp \frac{V'_{e_2}{}^{(4)}}{4!} \frac{\rho^4 \cos 5\phi}{2\sqrt{2}} + \frac{V'_{a_1}{}^{(4)}}{4!} \frac{\rho^4}{2\sqrt{2}} + \dots \quad (\text{A.5})$$

Similar expressions for the APES can be derived using a second and third order vibronic Hamiltonian, and are given in Table IX.

It can be seen that the APES only exhibits a dependence on  $\phi$  upon the inclusion of the fourth order vibronic coupling term, which translates to a five-fold degeneracy in the APES with respect to  $\phi$ . It is thus necessary to include the fourth order vibronic coupling term in order to explain the difference between the energies of the cyclopentadienyl radical with respect to the distortion along  $Q_\theta$  and  $Q_\epsilon$ . The pseudorotation barrier is then simply two times of this energy difference.

The vibronic coupling constants  $V'_{e_2}{}^{(1)}$  and  $V'_{e_2}{}^{(3)}$  can be obtained using the orbital vibronic coupling constants of the frontier orbitals directly (see Section II A). However, because of

the totally symmetric fourth order  $V_{a_1}^{(4)}$  term, the fourth order  $V_{e_2}^{(4)}$  term has to be derived as the difference of the fourth order orbital vibronic coupling constants of  $\psi_\theta$  and  $\psi_\epsilon$  with respect to  $Q_\theta$ . The constants with  $a_1'$  symmetry have to be obtained using the total energy of the system. However, as there have been some issues with regards to the reliability of the *GW* total energies of molecular systems,<sup>89,121,122</sup> we restrict the derivation of the  $a_1'$  vibronic coupling constants to the DFT and HF methods only.

## REFERENCES

- <sup>1</sup>H. Mustroph, "Potential-energy surfaces, the born-oppenheimer approximations, and the franck-condon principle: Back to the roots," *ChemPhysChem* **17**, 2616–2629 (2016).
- <sup>2</sup>H. Yang and M. W. Wong, "Automatic conformational search of transition states for catalytic reactions using genetic algorithm," *The Journal of Physical Chemistry A* **123**, 10303–10314 (2019).
- <sup>3</sup>D. L. Osborn, "Reaction mechanisms on multiwell potential energy surfaces in combustion (and atmospheric) chemistry," *Annual Review of Physical Chemistry* **68**, 233–260 (2017).
- <sup>4</sup>R. Lonsdale, J. N. Harvey, and A. J. Mulholland, "A practical guide to modelling enzyme-catalysed reactions," *Chemical Society Reviews* **41**, 3025 (2012).
- <sup>5</sup>N. Taricska, D. Horváth, D. K. Menyhárd, H. Ákontz-Kiss, M. Noji, M. So, Y. Goto, T. Fujiwara, and A. Perczel, "The route from the folded to the amyloid state: Exploring the potential energy surface of a drug-like miniprotein," *Chemistry - A European Journal* **26**, 1968–1978 (2019).
- <sup>6</sup>J. M. Rodgers, R. J. Hemley, and T. Ichiye, "Quasiharmonic analysis of protein energy landscapes from pressure-temperature molecular dynamics simulations," *The Journal of Chemical Physics* **147**, 125103 (2017).
- <sup>7</sup>P. Koehl, "Minimum action transition paths connecting minima on an energy surface," *The Journal of Chemical Physics* **145**, 184111 (2016).
- <sup>8</sup>R. A. Mata and M. A. Suhm, "Benchmarking quantum chemical methods: Are we heading in the right direction?" *Angewandte Chemie International Edition* **56**, 11011–11018 (2017).
- <sup>9</sup>I. B. Bersuker and V. Z. Polinger, *Vibronic Interactions in Molecules and Crystals* (Springer-Verlag Berlin Heidelberg, 1989).

- <sup>10</sup>G. Fischer, *Vibronic coupling: The Interaction Between the Electronic and Nuclear Motions*, Theoretical Chemistry: A Series of Monographs, Vol. 9 (Academic Press, 1984).
- <sup>11</sup>T. Azumi and K. Matsuzaki, “What does the term ”vibronic coupling” mean?” *Photochemistry and Photobiology* **25**, 315–326 (1977).
- <sup>12</sup>Z. Huang and D. Liu, “Dynamical jahn-teller effect in the first excited  $c_{60}^-$ ,” *International Journal of Quantum Chemistry* **120**, e26148 (2019).
- <sup>13</sup>D. Liu, Y. Niwa, N. Iwahara, T. Sato, and L. F. Chibotaru, “Quadratic jahn-teller effect of fullerene anions,” *Physical Review B* **98**, 035402 (2018).
- <sup>14</sup>F. Giustino, “Electron-phonon interactions from first principles,” *Reviews of Modern Physics* **89**, 015003 (2017).
- <sup>15</sup>L. Andjelković, M. Gruden-Pavlović, C. Daul, and M. Zlatar, “The choice of the exchange-correlation functional for the determination of the jahn-teller parameters by the density functional theory,” *International Journal of Quantum Chemistry* **113**, 859–864 (2013).
- <sup>16</sup>T. Sato, N. Iwahara, and K. Tanaka, “Critical reinvestigation of vibronic couplings in picene from view of vibronic coupling density analysis,” *Physical Review B* **85**, 161102(R) (2012).
- <sup>17</sup>M. Gruden-Pavlović, P. García-Fernández, L. Andjelković, C. Daul, and M. Zlatar, “Treatment of the multimode jahn-teller problem in small aromatic radicals,” *The Journal of Physical Chemistry A* **115**, 10801–10813 (2011).
- <sup>18</sup>J. L. Janssen, M. Côté, S. G. Louie, and M. L. Cohen, “Electron-phonon coupling in  $c_{60}$  using hybrid functionals,” *Physical Review B* **81**, 073106 (2010).
- <sup>19</sup>N. Iwahara, T. Sato, K. Tanaka, and L. F. Chibotaru, “Vibronic coupling in  $c_{60}^-$  anion revisited: Derivations from photoelectron spectra and DFT calculations,” *Physical Review B* **82**, 245409 (2010).
- <sup>20</sup>P. García-Fernández, I. B. Bersuker, J. A. Aramburu, M. T. Barriuso, and M. Moreno, “Origin of warping in the  $e \otimes e$  jahn-teller problem: Quadratic vibronic coupling versus anharmonicity and application to  $\text{NaCl} : \text{rh}^{2+}$  and triangular molecules,” *Physical Review B* **71**, 184117 (2005).
- <sup>21</sup>T. Kato and K. Hirao, “Vibronic interactions and jahn-teller effects in charged hydrocarbons,” (Elsevier, 2003) pp. 257–271.
- <sup>22</sup>T. Sato, K. Tokunaga, and K. Tanaka, “Vibronic coupling in cyclopentadienyl radical: A method for calculation of vibronic coupling constant and vibronic coupling density

- analysis,” *The Journal of Chemical Physics* **124**, 024314 (2006).
- <sup>23</sup>K. Tokunaga, T. Sato, and K. Tanaka, “Vibronic coupling in benzene cation and anion: Vibronic coupling and frontier electron density in jahn-teller molecules,” *The Journal of Chemical Physics* **124**, 154303 (2006).
- <sup>24</sup>H. Tachikawa, “Jahn-teller effect of the benzene radical cation: A direct ab initio molecular dynamics study,” *The Journal of Physical Chemistry A* **122**, 4121–4129 (2018).
- <sup>25</sup>N. Iwahara, V. Vieru, L. Ungur, and L. F. Chibotaru, “Zeeman interaction and jahn-teller effect in the  $\Gamma_8$  multiplet,” *Physical Review B* **96**, 064416 (2017).
- <sup>26</sup>Y. Liu, Y. Wang, and I. B. Bersuker, “Geometry, electronic structure, and pseudo jahn-teller effect in tetrasilacyclobutadiene analogues,” *Scientific Reports* **6**, 23315 (2016).
- <sup>27</sup>D. Opalka and W. Domcke, “High-order expansion of  $t_2 \times t_2$  jahn-teller potential-energy surfaces in tetrahedral molecules,” *The Journal of Chemical Physics* **132**, 154108 (2010).
- <sup>28</sup>K. Tokunaga, T. Sato, and K. Tanaka, “Calculation of vibronic coupling constant and vibronic coupling density analysis,” *Journal of Molecular Structure* **838**, 116–123 (2007).
- <sup>29</sup>S. Zilberg and Y. Haas, “A valence bond analysis of electronic degeneracies in jahn-teller systems: Low-lying states of the cyclopentadienyl radical and cation,” *Journal of the American Chemical Society* **124**, 10683–10691 (2002).
- <sup>30</sup>B. E. Applegate, T. A. Miller, and T. A. Barckholtz, “The jahn-teller and related effects in the cyclopentadienyl radical. i. the ab initio calculation of spectroscopically observable parameters,” *The Journal of Chemical Physics* **114**, 4855–4868 (2001).
- <sup>31</sup>J. H. Kiefer, R. S. Tranter, H. Wang, and A. F. Wagner, “Thermodynamic functions for the cyclopentadienyl radical: The effect of jahn-teller distortion,” *International Journal of Chemical Kinetics* **33**, 834–845 (2001).
- <sup>32</sup>M. J. Bearpark, M. A. Robb, and N. Yamamoto, “A cascf study of the cyclopentadienyl radical: conical intersections and the jahn-teller effect,” *Spectrochimica Acta Part A: Molecular and Biomolecular Spectroscopy* **55**, 639–646 (1999).
- <sup>33</sup>H. K. Tran, J. F. Stanton, and T. A. Miller, “Quantifying the effects of higher order coupling terms on fits using a second order jahn-teller hamiltonian,” *Journal of Molecular Spectroscopy* **343**, 102–115 (2018).
- <sup>34</sup>T. Ichino, S. W. Wren, K. M. Vogelhuber, A. J. Gianola, W. C. Lineberger, and J. F. Stanton, “The vibronic level structure of the cyclopentadienyl radical,” *The Journal of Chemical Physics* **129**, 084310 (2008).

- <sup>35</sup>T. Ichino, A. J. Gianola, W. C. Lineberger, and J. F. Stanton, “Nonadiabatic effects in the photoelectron spectrum of the pyrazolide-d3 anion: Three-state interactions in the pyrazolyl-d3 radical,” *The Journal of Chemical Physics* **125**, 084312 (2006).
- <sup>36</sup>S. Faraji, H. Köppel, W. Eisfeld, and S. Mahapatra, “Towards a higher-order description of jahn-teller coupling effects in molecular spectroscopy: The  $\tilde{A}^2E''$  state of  $\text{no}_3$ ,” *Chemical Physics* **347**, 110–119 (2008).
- <sup>37</sup>W. Eisfeld and A. Viel, “Higher order  $(a+e)\otimes e$  pseudo-jahn-teller coupling,” *The Journal of Chemical Physics* **122**, 204317 (2005).
- <sup>38</sup>A. Viel and W. Eisfeld, “Effects of higher order jahn-teller coupling on the nuclear dynamics,” *The Journal of Chemical Physics* **120**, 4603–4613 (2004).
- <sup>39</sup>A. Szabo and N. S. Ostlund, *Modern Quantum Chemistry: Introduction to Advanced Electronic Structure Theory* (Dover Publications, Inc., New York, 1996).
- <sup>40</sup>T. Koopmans, “Über die zuordnung von wellenfunktionen und eigenwerten zu den einzelnen elektronen eines atoms,” *Physica* **1**, 104–113 (1934).
- <sup>41</sup>B. O. Roos, R. Lindh, P. Å. Malmqvist, V. Veryazov, and P.-O. Widmark, *Multiconfigurational Quantum Chemistry* (John Wiley & Sons, Inc., 2016).
- <sup>42</sup>J. Olsen, “The casscf method: A perspective and commentary,” *International Journal of Quantum Chemistry* **111**, 3267–3272 (2011).
- <sup>43</sup>K. Yamaguchi, S. Yamanaka, J. Shimada, H. Isobe, T. Saito, M. Shoji, Y. Kitagawa, and M. Okumura, “Extended hartree-fock theory of chemical reactions. IX. diradical and perepoxide mechanisms for oxygenations of ethylene with molecular oxygen and iron-oxo species are revisited,” *International Journal of Quantum Chemistry* **109**, 3745–3766 (2009).
- <sup>44</sup>Y. Jung and M. Head-Gordon, “How diradicaloid is a stable diradical?” *ChemPhysChem* **4**, 522–525 (2003).
- <sup>45</sup>L. Ungur and L. F. Chibotaru, “Computational modelling of the magnetic properties of lanthanide compounds,” in *Lanthanides and Actinides in Molecular Magnetism* (John Wiley & Sons, Ltd, 2015) pp. 153–184.
- <sup>46</sup>J. P. Perdew, K. Burke, and M. Ernzerhof, “Generalized gradient approximation made simple,” *Physical Review Letters* **77**, 3865–3868 (1996).
- <sup>47</sup>Y. Zhao and D. G. Truhlar, “The m06 suite of density functionals for main group thermochemistry, thermochemical kinetics, noncovalent interactions, excited states, and tran-

- sition elements: two new functionals and systematic testing of four m06-class functionals and 12 other functionals,” *Theoretical Chemistry Accounts* **120**, 215–241 (2007).
- <sup>48</sup>A. D. Becke, “Density-functional thermochemistry. III. the role of exact exchange,” *The Journal of Chemical Physics* **98**, 5648–5652 (1993).
- <sup>49</sup>P. J. Stephens, F. J. Devlin, C. F. Chabalowski, and M. J. Frisch, “Ab initio calculation of vibrational absorption and circular dichroism spectra using density functional force fields,” *The Journal of Physical Chemistry* **98**, 11623–11627 (1994).
- <sup>50</sup>N. Mardirossian and M. Head-Gordon, “Thirty years of density functional theory in computational chemistry: an overview and extensive assessment of 200 density functionals,” *Molecular Physics* **115**, 2315–2372 (2017).
- <sup>51</sup>R. O. Jones, “Density functional theory: Its origins, rise to prominence, and future,” *Reviews of Modern Physics* **87**, 897–923 (2015).
- <sup>52</sup>A. D. Becke, “Perspective: Fifty years of density-functional theory in chemical physics,” *The Journal of Chemical Physics* **140**, 18A301 (2014).
- <sup>53</sup>R. M. Martin, L. Reining, and D. M. Ceperley, *Interacting Electrons: Theory and Computational Approaches* (Cambridge University Press, 2016).
- <sup>54</sup>F. Bechstedt, *Many-Body Approach to Electronic Excitations* (Springer-Verlag Berlin Heidelberg, 2015) p. 584.
- <sup>55</sup>L. Reining, “The *gw* approximation: content, successes and limitations,” *WIREs Computational Molecular Science* **8** (2017), 10.1002/wcms.1344.
- <sup>56</sup>L. Hedin, “New method for calculating the one-particle green’s function with application to the electron-gas problem,” *Physical Review* **139**, A796–A823 (1965).
- <sup>57</sup>G. Onida, L. Reining, and A. Rubio, “Electronic excitations: density-functional versus many-body green’s-function approaches,” *Reviews of Modern Physics* **74**, 601–659 (2002).
- <sup>58</sup>L. Hedin, “On correlation effects in electron spectroscopies and the *gw* approximation,” *Journal of Physics: Condensed Matter* **11**, R489–R528 (1999).
- <sup>59</sup>Z. B. Maksić and R. Vianello, “How good is koopmans’ approximation? *g2(mp2)* study of the vertical and adiabatic ionization potentials of some small molecules,” *The Journal of Physical Chemistry A* **106**, 6515–6520 (2002).
- <sup>60</sup>P. Politzer and F. Abu-Awwad, “A comparative analysis of hartree-fock and kohn-sham orbital energies,” *Theoretical Chemistry Accounts: Theory, Computation, and Modeling (Theoretica Chimica Acta)* **99**, 83–87 (1998).

- <sup>61</sup>L. Gallandi, N. Marom, P. Rinke, and T. Körzdörfer, “Accurate ionization potentials and electron affinities of acceptor molecules ii: Non-empirically tuned long-range corrected hybrid functionals,” *Journal of Chemical Theory and Computation* **12**, 605–614 (2016).
- <sup>62</sup>M. J. van Setten, F. Caruso, S. Sharifzadeh, X. Ren, M. Scheffler, F. Liu, J. Lischner, L. Lin, J. R. Deslippe, S. G. Louie, C. Yang, F. Weigend, J. B. Neaton, F. Evers, and P. Rinke, “*gw*100: Benchmarking  $g_0w_0$  for molecular systems,” *Journal of Chemical Theory and Computation* **11**, 5665–5687 (2015).
- <sup>63</sup>M. J. van Setten, F. Weigend, and F. Evers, “The *gw*-method for quantum chemistry applications: Theory and implementation,” *Journal of Chemical Theory and Computation* **9**, 232–246 (2012).
- <sup>64</sup>X. Ren, P. Rinke, V. Blum, J. Wieferink, A. Tkatchenko, A. Sanfilippo, K. Reuter, and M. Scheffler, “Resolution-of-identity approach to hartree-fock, hybrid density functionals, rpa, mp2 and *gw* with numeric atom-centered orbital basis functions,” *New Journal of Physics* **14**, 053020 (2012).
- <sup>65</sup>F. Bruneval and M. A. L. Marques, “Benchmarking the starting points of the *gw* approximation for molecules,” *Journal of Chemical Theory and Computation* **9**, 324–329 (2013).
- <sup>66</sup>X. Blase, C. Attaccalite, and V. Olevano, “First-principles *gw* calculations for fullerenes, porphyrins, phtalocyanine, and other molecules of interest for organic photovoltaic applications,” *Physical Review B* **83**, 115103 (2011).
- <sup>67</sup>C. Faber, C. Attaccalite, V. Olevano, E. Runge, and X. Blase, “First-principles *gw* calculations for dna and rna nucleobases,” *Physical Review B* **83**, 115123 (2011).
- <sup>68</sup>C. Faber, J. L. Janssen, M. Côté, E. Runge, and X. Blase, “Electron-phonon coupling in the C<sub>60</sub> fullerene within the many-body *GW* approach,” *Physical Review B* **84**, 155104 (2011).
- <sup>69</sup>Z. Li, G. Antonius, M. Wu, F. H. da Jornada, and S. G. Louie, “Electron-phonon coupling from *Ab Initio* linear-response theory within the *gw* method: Correlation-enhanced interactions and superconductivity in  $ba_{1-x}k_xbio_3$ ,” *Physical Review Letters* **122**, 186402 (2019).
- <sup>70</sup>P. Koval, M. P. Ljungberg, M. Müller, and D. Sánchez-Portal, “Toward efficient *gw* calculations using numerical atomic orbitals: Benchmarking and application to molecular dynamics simulations,” *Journal of Chemical Theory and Computation* **15**, 4564–4580

(2019).

- <sup>71</sup>F. Karsai, M. Engel, E. Flage-Larsen, and G. Kresse, “Electron-phonon coupling in semiconductors within the *gw* approximation,” *New Journal of Physics* **20**, 123008 (2018).
- <sup>72</sup>C. Faber, P. Boulanger, C. Attaccalite, E. Cannuccia, I. Duchemin, T. Deutsch, and X. Blase, “Exploring approximations to the *gw* self-energy ionic gradients,” *Physical Review B* **91**, 155109 (2015).
- <sup>73</sup>C. Faber, I. Duchemin, T. Deutsch, C. Attaccalite, V. Olevano, and X. Blase, “Electron-phonon coupling and charge-transfer excitations in organic systems from many-body perturbation theory,” *Journal of Materials Science* **47**, 7472–7481 (2012).
- <sup>74</sup>B. E. Applegate, A. J. Bezant, and T. A. Miller, “The jahn-teller and related effects in the cyclopentadienyl radical. ii. vibrational analysis of the  $\tilde{a}^2A_2'' - \tilde{x}^2E_1''$  electronic transition,” *The Journal of Chemical Physics* **114**, 4869–4882 (2001).
- <sup>75</sup>K. Sharma, S. Garner, T. A. Miller, and J. F. Stanton, “First-principles calculation of jahn-teller rotational distortion parameters,” *The Journal of Physical Chemistry A* **123**, 4990–5004 (2019).
- <sup>76</sup>M. Shapero, I. A. Ramphal, and D. M. Neumark, “Photodissociation of the cyclopentadienyl radical at 248 nm,” *The Journal of Physical Chemistry A* **122**, 4265–4272 (2018).
- <sup>77</sup>D. Leicht, M. Kaufmann, G. Schwaab, and M. Havenith, “Infrared spectroscopy of the helium solvated cyclopentadienyl radical in the ch stretch region,” *The Journal of Chemical Physics* **145**, 074304 (2016).
- <sup>78</sup>C. Cunha and S. Canuto, “Ground state structure of  $c_5h_5$  and van der waals interaction with he and ne,” *Journal of Molecular Structure: THEOCHEM* **464**, 73–77 (1999).
- <sup>79</sup>W. Zou, M. Filatov, and D. Cremer, “Bondpseudorotation, jahn-teller, and pseudo-jahn-teller effects in the cyclopentadienyl cation and its pentahalogeno derivatives,” *International Journal of Quantum Chemistry* **112**, 3277–3288 (2012).
- <sup>80</sup>H. J. Wörner and F. Merkt, “Jahn-teller effects in molecular cations studied by photoelectron spectroscopy and group theory,” *Angewandte Chemie International Edition* **48**, 6404–6424 (2009).
- <sup>81</sup>H. J. Wörner and F. Merkt, “Diradicals, antiaromaticity, and the pseudo-jahn-teller effect: Electronic and rovibronic structures of the cyclopentadienyl cation,” *The Journal of Chemical Physics* **127**, 034303 (2007).
- <sup>82</sup>I. V. Tokmakov, L. V. Moskaleva, and M.-C. Lin, “Quantum chemical/vRRKM study

- on the thermal decomposition of cyclopentadiene,” *International Journal of Chemical Kinetics* **36**, 139–151 (2004).
- <sup>83</sup>G. Katzer and A. F. Sax, “Numerical determination of pseudorotation constants,” *The Journal of Chemical Physics* **117**, 8219–8228 (2002).
- <sup>84</sup>A. D. Liehr, “Topological aspects of the conformational stability problem. part i. degenerate electronic states,” *The Journal of Physical Chemistry* **67**, 389–471 (1963).
- <sup>85</sup>T. Inui, Y. Tanabe, and Y. Onodera, *Group Theory and Its Applications in Physics* (Springer-Verlag Berlin Heidelberg, Berlin and Heidelberg, 1990).
- <sup>86</sup>S. L. Altmann and P. Herzog, *Point-Group Theory Tables*, 2nd ed. (Clarendon Press, Oxford, 2011).
- <sup>87</sup>H. A. Jahn and E. Teller, “Stability of polyatomic molecules in degenerate electronic states - i-orbital degeneracy,” *Proceedings of the Royal Society of London. Series A - Mathematical and Physical Sciences* **161**, 220–235 (1937).
- <sup>88</sup>I. B. Bersuker, “Limitations of density functional theory in application to degenerate states,” *Journal of Computational Chemistry* **18**, 260–267 (1997).
- <sup>89</sup>D. Golze, M. Dvorak, and P. Rinke, “The gw compendium: A practical guide to theoretical photoemission spectroscopy,” *Frontiers in Chemistry* **7** (2019), 10.3389/fchem.2019.00377.
- <sup>90</sup>C. Adamo and V. Barone, “Toward reliable density functional methods without adjustable parameters: The PBE0 model,” *The Journal of Chemical Physics* **110**, 6158–6170 (1999).
- <sup>91</sup>T. H. Dunning, “Gaussian basis sets for use in correlated molecular calculations. i. the atoms boron through neon and hydrogen,” *The Journal of Chemical Physics* **90**, 1007–1023 (1989).
- <sup>92</sup>M. J. Frisch, G. W. Trucks, H. B. Schlegel, G. E. Scuseria, M. A. Robb, J. R. Cheeseman, G. Scalmani, V. Barone, G. A. Petersson, H. Nakatsuji, X. Li, M. Caricato, A. V. Marenich, J. Bloino, B. G. Janesko, R. Gomperts, B. Mennucci, H. P. Hratchian, J. V. Ortiz, A. F. Izmaylov, J. L. Sonnenberg, D. Williams-Young, F. Ding, F. Lipparini, F. Egidi, J. Goings, B. Peng, A. Petrone, T. Henderson, D. Ranasinghe, V. G. Zakrzewski, J. Gao, N. Rega, G. Zheng, W. Liang, M. Hada, M. Ehara, K. Toyota, R. Fukuda, J. Hasegawa, M. Ishida, T. Nakajima, Y. Honda, O. Kitao, H. Nakai, T. Vreven, K. Throssell, J. A. Montgomery, Jr., J. E. Peralta, F. Ogliaro, M. J. Bearpark, J. J. Heyd, E. N. Brothers, K. N. Kudin, V. N. Staroverov, T. A. Keith, R. Kobayashi, J. Normand, K. Raghavachari, A. P. Rendell, J. C. Burant, S. S. Iyengar, J. Tomasi, M. Cossi, J. M. Millam, M. Klene,

- C. Adamo, R. Cammi, J. W. Ochterski, R. L. Martin, K. Morokuma, O. Farkas, J. B. Foresman, and D. J. Fox, "Gaussian16 Revision A.01," (2016), gaussian Inc. Wallingford CT.
- <sup>93</sup>T. D. Kühne, M. Iannuzzi, M. D. Ben, V. V. Rybkin, P. Seewald, F. Stein, T. Laino, R. Z. Khaliullin, O. Schütt, F. Schiffmann, D. Golze, J. Wilhelm, S. Chulkov, M. H. Bani-Hashemian, V. Weber, U. Borštnik, M. Taillefumier, A. S. Jakobovits, A. Lazzaro, H. Pabst, T. Müller, R. Schade, M. Guidon, S. Andermatt, N. Holmberg, G. K. Schenter, A. Hehn, A. Bussy, F. Belleflamme, G. Tabacchi, A. Glöβ, M. Lass, I. Bethune, C. J. Mundy, C. Plessl, M. Watkins, J. VandeVondele, M. Krack, and J. Hutter, "Cp2k: An electronic structure and molecular dynamics software package – quickstep: Efficient and accurate electronic structure calculations," (2020), arXiv:2003.03868 [physics.chem-ph].
- <sup>94</sup>J. Hutter, M. Iannuzzi, F. Schiffmann, and J. VandeVondele, "cp2k: atomistic simulations of condensed matter systems," *Wiley Interdisciplinary Reviews: Computational Molecular Science* **4**, 15–25 (2013).
- <sup>95</sup>O. A. Vydrov and G. E. Scuseria, "Assessment of a long-range corrected hybrid functional," *The Journal of Chemical Physics* **125**, 234109 (2006).
- <sup>96</sup>J.-D. Chai and M. Head-Gordon, "Systematic optimization of long-range corrected hybrid density functionals," *The Journal of Chemical Physics* **128**, 084106 (2008).
- <sup>97</sup>J.-D. Chai and M. Head-Gordon, "Long-range corrected hybrid density functionals with damped atom-atom dispersion corrections," *Physical Chemistry Chemical Physics* **10**, 6615 (2008).
- <sup>98</sup>T. Yanai, D. P. Tew, and N. C. Handy, "A new hybrid exchange-correlation functional using the coulomb-attenuating method (cam-b3lyp)," *Chemical Physics Letters* **393**, 51–57 (2004).
- <sup>99</sup>J. Autschbach and M. Srebro, "Delocalization error and "functional tuning" in kohn-sham calculations of molecular properties," *Accounts of Chemical Research* **47**, 2592–2602 (2014).
- <sup>100</sup>L. Kronik, T. Stein, S. Refaely-Abramson, and R. Baer, "Excitation gaps of finite-sized systems from optimally tuned range-separated hybrid functionals," *Journal of Chemical Theory and Computation* **8**, 1515–1531 (2012).
- <sup>101</sup>R. Baer, E. Livshits, and U. Salzner, "Tuned range-separated hybrids in density functional theory," *Annual Review of Physical Chemistry* **61**, 85–109 (2010).

- <sup>102</sup>T. Stein, L. Kronik, and R. Baer, “Reliable prediction of charge transfer excitations in molecular complexes using time-dependent density functional theory,” *Journal of the American Chemical Society* **131**, 2818–2820 (2009).
- <sup>103</sup>T. Stein, L. Kronik, and R. Baer, “Prediction of charge-transfer excitations in coumarin-based dyes using a range-separated functional tuned from first principles,” *The Journal of Chemical Physics* **131**, 244119 (2009).
- <sup>104</sup>J. Bois and T. Körzdörfer, “Size-dependence of nonempirically tuned DFT starting points for  $g_0w_0$  applied to  $\pi$ -conjugated molecular chains,” *Journal of Chemical Theory and Computation* **13**, 4962–4971 (2017).
- <sup>105</sup>L. Gallandi and T. Körzdörfer, “Long-range corrected DFT meets  $gw$ : Vibrationally resolved photoelectron spectra from first principles,” *Journal of Chemical Theory and Computation* **11**, 5391–5400 (2015).
- <sup>106</sup>F. Weigend, A. Köhn, and C. Hättig, “Efficient use of the correlation consistent basis sets in resolution of the identity MP2 calculations,” *The Journal of Chemical Physics* **116**, 3175–3183 (2002).
- <sup>107</sup>J. Wilhelm, M. D. Ben, and J. Hutter, “ $gw$  in the gaussian and plane waves scheme with application to linear acenes,” *Journal of Chemical Theory and Computation* **12**, 3623–3635 (2016).
- <sup>108</sup>B. P. Pritchard, D. Altarawy, B. Didier, T. D. Gibson, and T. L. Windus, “New basis set exchange: An open, up-to-date resource for the molecular sciences community,” *Journal of Chemical Information and Modeling* **59**, 4814–4820 (2019).
- <sup>109</sup>P.-K. Lo and K.-C. Lau, “High-level *ab Initio* predictions for the ionization energy, electron affinity, and heats of formation of cyclopentadienyl radical, cation, and anion,  $c_5h_5/c_5h_5^+/c_5h_5^-$ ,” *The Journal of Physical Chemistry A* **118**, 2498–2507 (2014).
- <sup>110</sup>E. Maggio, P. Liu, M. J. van Setten, and G. Kresse, “ $gw100$ : A plane wave perspective for small molecules,” *Journal of Chemical Theory and Computation* **13**, 635–648 (2017).
- <sup>111</sup>J. P. Perdew and A. Zunger, “Self-interaction correction to density-functional approximations for many-electron systems,” *Physical Review B* **23**, 5048–5079 (1981).
- <sup>112</sup>P. Mori-Sánchez, A. J. Cohen, and W. Yang, “Many-electron self-interaction error in approximate density functionals,” *The Journal of Chemical Physics* **125**, 201102 (2006).
- <sup>113</sup>A. Ruzsinszky, J. P. Perdew, G. I. Csonka, O. A. Vydrov, and G. E. Scuseria, “Spurious fractional charge on dissociated atoms: Pervasive and resilient self-interaction error of

- common density functionals,” *The Journal of Chemical Physics* **125**, 194112 (2006).
- <sup>114</sup>A. J. Cohen, P. Mori-Sánchez, and W. Yang, “Challenges for density functional theory,” *Chemical Reviews* **112**, 289–320 (2011).
- <sup>115</sup>J. F. Stanton and J. Gauss, “Analytic energy derivatives for ionized states described by the equation-of-motion coupled cluster method,” *The Journal of Chemical Physics* **101**, 8938–8944 (1994).
- <sup>116</sup>A. I. Krylov, “Equation-of-motion coupled-cluster methods for open-shell and electronically excited species: The hitchhiker’s guide to fock space,” *Annual Review of Physical Chemistry* **59**, 433–462 (2008).
- <sup>117</sup>J. F. Stanton, “Coupled-cluster theory, pseudo-jahn-teller effects and conical intersections,” *The Journal of Chemical Physics* **115**, 10382 (2001).
- <sup>118</sup>R. J. Bartlett, “How and why coupled-cluster theory became the pre-eminent method in an ab initio quantum chemistry,” in *Theory and Applications of Computational Chemistry*, edited by C. E. Dykstra, G. Frenking, K. S. Kim, and G. E. Scuseria (Elsevier, Amsterdam, 2005) pp. 1191–1221.
- <sup>119</sup>J. Noga and R. J. Bartlett, “The full ccsdt model for molecular electronic structure,” *The Journal of Chemical Physics* **86**, 7041–7050 (1987).
- <sup>120</sup>J. D. Watts, J. Gauss, and R. J. Bartlett, “Coupled-cluster methods with noniterative triple excitations for restricted open-shell hartree-fock and other general single determinant reference functions. energies and analytical gradients,” *The Journal of Chemical Physics* **98**, 8718–8733 (1993).
- <sup>121</sup>F. Caruso, P. Rinke, X. Ren, M. Scheffler, and A. Rubio, “Unified description of ground and excited states of finite systems: The self-consistent gw approach,” *Physical Review B* **86** (2012), 10.1103/physrevb.86.081102.
- <sup>122</sup>A. Stan, N. E. Dahlen, and R. van Leeuwen, “Levels of self-consistency in the gw approximation,” *The Journal of Chemical Physics* **130**, 114105 (2009).